CHAPTER 5

MILLING CIRCUIT CONTROL SIMULATION STUDY

This chapter details simulation results of applying the RNMPC of Section 3.7, NMPC and single-loop PI controllers of Section 4.5 to the milling circuit model of Section 2.3.4. The objectives for milling control are presented in Section 1.2. The performance metrics are described before the main results of the simulation study are presented. A summary of the different simulation scenarios together with the performance values are provided at the end of this chapter.

5.1 INTRODUCTION

In this simulation study, RNMPC is compared to NMPC and single-loop PI controllers for different operational conditions. In all the simulations, severe parameter uncertainty is employed.

The simulations all assume that the process is operating under normal operating conditions before the disturbances are introduced at time $t = 0$. The normal operating condition of the milling circuit can be obtained from the circuit mathematical model known as the nominal operating point.

The nominal operating point of the model is obtained by applying the nominal parameters ($\tilde{\mathbf{p}}$) for the milling circuit to the model and calculating the state ($\mathbf{x_0}$) and input ($\mathbf{u_0}$) values that result in the rate-of-change of the states being zero ($\frac{\partial x_i}{\partial t} = 0, \forall i = 1, 2, \ldots, n$ where n is the number of states). The system will therefore remain at the current operating condition (state) if the inputs remain constant and there is no external disturbance acting on it.

A constrained nonlinear optimisation is performed with regard to the states x and inputs u that lead to zero state variation $\frac{\partial x}{\partial t} = 0$ to obtain the nominal operating point. Constraints are defined such that the operating point will be physically relevant, e.g. there are no negative feed-rates, power-draw or holdup of material in the mill or sump. Table 5.1 details the constraints (Min and Max), the calculated operating point value (OP) and the objective function weighting (W) for all the states, manipulated variables and controlled variables of the milling circuit model. If a variable is not included in the objective function, it is indicated by "—" in the weightings column (W), otherwise, if the variable is present in the objective function, but not penalised, it is indicated by "0" in the weightings column (W).

The milling circuit model contains large parameter uncertainties; this is especially true of the parameters related to the composition of the feed-ore and the hardness of the ore, which has an impact on the energy needed to grind a ton of ore. The parameter vector changes every 200 seconds, to allow the parameter disturbances to sufficiently impact the simulation. The aim of these relatively fast changes is to simulate the natural variation of the feed. The parameters follow a uniform distribution to produce large changes in the parameter values in order to properly demonstrate the disturbance rejection capabilities of the controller.

Feed ore hardness and composition changes are major disturbances that milling circuit controllers have to contend with, especially when the feed ore is switched between feeds that originate from different stockpiles. A feed ore hardness increase is simulated by increasing the power needed to produce a ton of fines (ϕ_f) by 50% in some of the simulation scenarios. A feed ore composition change is simulated by increasing the fraction of the feed consisting of rock (α_r) by 50% in some of the simulation scenarios. These disturbances are very large but not uncommon in practice.

The nominal, minimum and maximum values as well as the percentage variation of all the model parameters are detailed in Table 5.2. Figure 5.1 shows an example of typical parameter variations graphically, as employed in the simulations.

5.2 PERFORMANCE METRICS

The metrics in this section help quantify the performance of the controllers in terms of the economic objectives stated in Section 1.2 and the tracking performance of the LOAD. The two main economic objectives considered in this thesis are PSE tracking (objective 1b) and average throughput (objective 2). PSE setpoint tracking performance is calculated as

$$\mathrm{PSE}_{\mathrm{performance}} \triangleq \sum_{k=0}^{T_{sim}/\tau_s} \left(\mathrm{PSE}(k) - \bar{\mathrm{PSE}}(k)\right)^2 \tag{5.1}$$

where T_{sim} is the simulation time, τ_s is the sampling time, $\mathrm{PSE}(k)$ is the product particle size at sample k and $\bar{\mathrm{PSE}}(k)$ is the setpoint for particle size at sample k. Average throughput is calculated by

$$\mathrm{THROUGHPUT}_{\mathrm{average}} \triangleq \frac{1}{N} \sum_{k=0}^{N=T_{sim}/\tau_s} \mathrm{THROUGHPUT}(k) \tag{5.2}$$

Table 5.1: Constraints (Min, Max, Δ), operating point (OP) and objective function weighting (W).

Variable	Min	Max	Δ	OP	W	Description
X_{mw}	0	50	—	8.53	—	The holdup of water in the mill. [m^3]
X_{ms}	0	50	—	9.47	—	The holdup of ore in the mill. [m^3]
X_{mf}	0	50	—	3.54	—	The holdup of fine ore in the mill. [m^3]
X_{mr}	0	50	—	20.25	—	The holdup of rocks in the mill. [m^3]
X_{mb}	0	20	—	6.75	—	The holdup of balls in the mill. [m^3]
X_{sw}	0	10	—	3.95	—	The holdup of water in the sump. [m^3]
X_{ss}	0	10	—	1.05	—	The holdup of ore in the sump. [m^3]
X_{sf}	0	10	—	0.14	—	The holdup of fine ore in the sump. [m^3]
MIW	0	100	10	33.33	0.01	The flow-rate of water to the circuit. [$m^3/hour$]
MFS	0	200	10	100	0.01	The flow-rate of ore to the circuit (consists of rocks, coarse and fine ore). [$tons/hour$]
MFB	0	4	1	2	0.01	The flow-rate of balls to the circuit. [$tons/hour$]
α_{speed}	0.7	1.0	—	0.82	—	The fraction of critical mill speed.
CFF	400	500	—	443	0.01	The flow-rate of water from the sump to the cyclone. [$m^3/hour$]
SFW	0	400	—	267	0.01	The flow-rate of extra water to the sump. [$m^3/hour$]
PSE	60	90	—	80	100	Product particle-size. [$\% < 75\mu m$]
LOAD	30	50	—	45	100	The total charge of the mill. [%]
SLEV	2	9.5	—	5.0	0	The level of the sump. [m^3]
Γ	0	1	—	0.51	0	Rheology Factor.
THROUGHPUT	100	0	—	200	1	Product throughput consisting of coarse and fine solids. [$tons/hour$]
P_{mill}	0	2000	—	2000	0	Power draw of the mill motor. [kW]

Table 5.2: Nominal, minimum and maximum parameter values for a closed-circuit ROM milling circuit.

Parm	Nom	Min	Max	%Δ	Description
α_f	0.1	0.05	0.15	50	Fraction of fines in the ore. [dimensionless]
α_r	0.1	0.05	0.15	50	Fraction of rocks in the ore. [dimensionless]
ϕ_f	28	14	42	50	Power per fines produced. [$^{\text{kW}\cdot\text{hr}}/_{\text{ton}}$]
ϕ_r	69	55	83	20	Rock abrasion factor. [$^{\text{kW}\cdot\text{hr}}/_{\text{ton}}$]
ϕ_b	94	89	99	5	Steel abrasion factor. [$^{\text{kW}\cdot\text{hr}}/_{\text{ton}}$]
P_{max}	2000	—	—	—	Maximum mill motor power. [kW]
υ_{mill}	100	—	—	—	Mill volume. [m^3]
$\upsilon_{P_{\text{max}}}$	0.45	—	—	—	Fraction of mill volume filled for maximum power. [dimensionless]
$\Gamma_{P_{\text{max}}}$	0.51	—	—	—	Rheology factor for maximum mill power. [dimensionless]
ε_{ws}	0.6	—	—	—	Maximum water-to-solids volumetric ratio at zero pulp flow. [dimensionless]
V_V	40	—	—	—	Volumetric flow per “flowing volume” driving force. [hr^{-1}]
δ_{Pv}	1	—	—	—	Power-change parameter for volume. [dimensionless]
δ_{Ps}	1	—	—	—	Power-change parameter for fraction solids. [dimensionless]
α_P	0.82	—	—	—	Fractional power reduction per fractional reduction from maximum mill speed. [dimensionless]
α_{ϕ_f}	0.01	—	—	—	Fractional change in kW/fines produced per change in fractional filling of mill. [dimensionless]
χ_P	0	—	—	—	Cross-term for maximum power. [dimensionless]
ε_c	184	175	193	5	Cyclone coarse split. [dimensionless]
α_{su}	0.16	0.15	0.17	5	Fraction of solids in the underflow of the cyclone. [dimensionless]
C_1	0.6	—	—	—	Constant. [dimensionless]
C_2	0.7	—	—	—	Constant. [dimensionless]
C_3	3	—	—	—	Constant. [dimensionless]
C_4	3	—	—	—	Constant. [dimensionless]

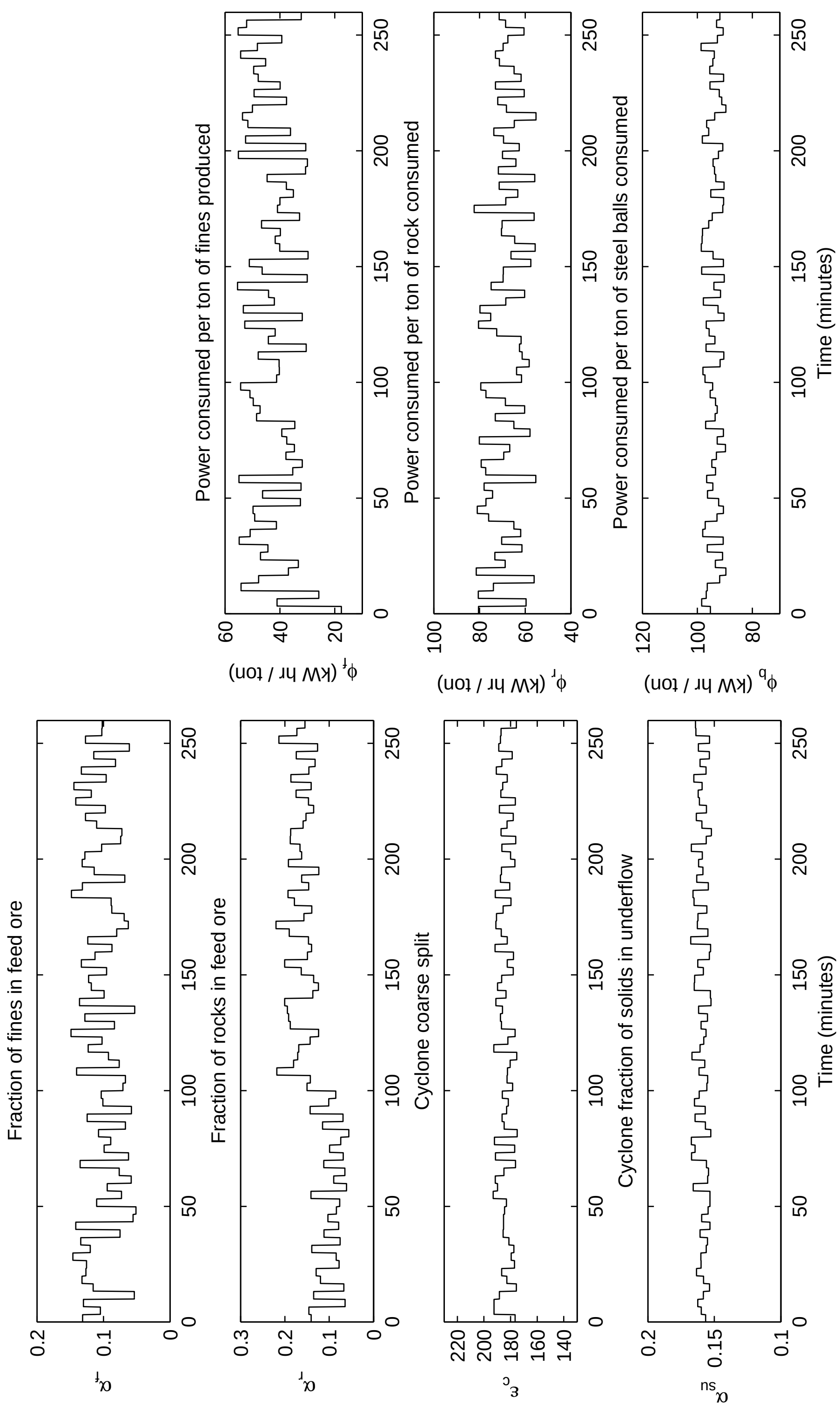

(a) Feed ore composition and cyclone split characteristics.

(b) Ore and steel balls hardness.

Figure 5.1: Parameter variations for nonlinear model.

where N is the total number of samples in the simulation and $\text{THROUGHPUT}(k)$ is the throughput of the milling circuit at sample k.

The LOAD setpoint tracking performance is calculated as

$$\text{LOAD}_{\text{tracking}} \triangleq \sum_{k=0}^{T_{sim}/\tau_s} \left(\text{LOAD}(k) - \bar{\text{LOAD}}(k)\right)^2 \tag{5.3}$$

where $\text{LOAD}(k)$ is the volumetric filling of the mill at sample k and $\bar{\text{LOAD}}(k)$ is the setpoint for the volumetric filling of the mill at sample k, which is similar to the calculation for PSE tracking performance.

The stage cost of the objective function (3.95) used for the simulations in this chapter and Addendum B is given by

$$L_i(s_i, q_i) \triangleq \begin{bmatrix} \text{PSE} \\ \text{LOAD} \\ \text{SLEV} \\ \text{THROUGHPUT} \\ \text{Rheology} \\ \text{Mill Power} \end{bmatrix}^T Q \begin{bmatrix} \text{PSE} \\ \text{LOAD} \\ \text{SLEV} \\ \text{THROUGHPUT} \\ \text{Rheology} \\ \text{Mill Power} \end{bmatrix} + \begin{bmatrix} \Delta\text{CFF} \\ \Delta\text{MFS} \\ \Delta\text{SFW} \\ \Delta\text{MIW} \\ \Delta\text{Balls} \end{bmatrix}^T R \begin{bmatrix} \Delta\text{CFF} \\ \Delta\text{MFS} \\ \Delta\text{SFW} \\ \Delta\text{MIW} \\ \Delta\text{Balls} \end{bmatrix} \tag{5.4}$$

where Q and R are diagonal matrices and the diagonal entries are given in the "W" columns of Table 5.4. An example of a typical Q matrix is given by

$$Q = \begin{bmatrix} \mathbf{100} & 0 & 0 & 0 & 0 & 0 \\ 0 & \mathbf{100} & 0 & 0 & 0 & 0 \\ 0 & 0 & \mathbf{1} & 0 & 0 & 0 \\ 0 & 0 & 0 & \mathbf{0} & 0 & 0 \\ 0 & 0 & 0 & 0 & \mathbf{0} & 0 \\ 0 & 0 & 0 & 0 & 0 & \mathbf{0} \end{bmatrix} \tag{5.5}$$

and a typical R matrix is given by

$$R = \begin{bmatrix} \mathbf{0.1} & 0 & 0 & 0 & 0 \\ 0 & \mathbf{0.1} & 0 & 0 & 0 \\ 0 & 0 & \mathbf{0.1} & 0 & 0 \\ 0 & 0 & 0 & \mathbf{0.1} & 0 \\ 0 & 0 & 0 & 0 & \mathbf{0.1} \end{bmatrix} \tag{5.6}$$

where the bold entries are given in Table 5.4 for the different simulation scenarios.

The NMPC and RNMPC controllers allow any arbitrary form for the objective function and does not have to follow the form of equation (3.95). Alternative forms of the objective function can potentially express certain performance criteria more naturally. Alternative forms of the objective function should, however, be verified not to affect the convergence and speed of the controller to the point where the controller becomes impractical.

5.3 SIMULATION RESULTS

This section details the simulation results of applying the RNMPC and NMPC of Section 3.7 and the single-loop PI controllers of Section 4.5 to the milling circuit model of Section 2.3.4.

5.3.1 Simulation parameters

This section outlines the sampling interval, prediction horizon and control horizon or nodes used by the both the RNMPC and NMPC controllers and the length of the simulations used by all the controllers, as shown in Table 5.3.

Process time constants for the dynamics that relate the MFS to LOAD and PSE are in the order of thirty minutes, whereas the time constants relating CFF and SFW to PSE are in the order of one or two minutes. Hence a sampling time of 10 seconds is recommended in Craig and MacLeod (1995). An additional motivation for this choice of sampling time is that during normal operation the sump volume is about 5 cubic metres and the flow rates of CFF and SFW range from 400 to 500 $^{m^3}/_{hour}$ and 0 to 400 $^{m^3}/_{hour}$ respectively. If, for example, the difference between CFF and SFW is 300 $^{m^3}/_{hour}$, the sump will run dry or overflow within about one minute.

The current implementation of the RNMPC and NMPC uses the same length of time for both the prediction and control horizons. It expresses the prediction and control horizons in multiples of the sampling time, which is 10 seconds for all the simulations. The prediction and control horizons are chosen to be 6 sampling intervals for all the simulations, thus 60 seconds. The number of nodes specifies the number of control vectors that is calculated over the control horizon. The number of nodes is also set to 6 for all the simulations, resulting in a control vector being calculated every 10 seconds over the control horizon. If, for example, the prediction and control horizons were set to 120 seconds and the number of nodes remained at 6, a control vector would have been calculated every 20 seconds over the length of the control horizon.

The weighting of the variables in Q and R of equation (3.96) is described by the “W” column in Table 5.1 and chosen based on the performance criteria of Section 1.2. Further, $P = Q$ with no terminal constraints ($\theta_N(s_N) \in \mathbb{R}^{N_x}$). The inputs are normalised according to their maximum range and outputs are normalised according to their setpoints in the objective function.

Figure 5.2 and Figure 5.3 show that the variables of interest, namely PSE, LOAD, SLEV, MFS and THROUGHPUT, reach steady-state within about 250 minutes. Other variables,

Table 5.3: Simulation Parameter Summary.

Variable	Value	Variable	Value
Prediction & Control Horizons (T)	60 seconds	Nodes (N)	6
Terminal Constraints ($\theta_N(s_N)$)	None ($\mathbb{R}^{N_x}$)	Simulation time	260 minutes
Terminal Cost Weighting (P)	Q	Sampling Time (τ_s)	10 seconds

such as MFB, take much longer to reach steady-state, but do not seem to have an impact on PSE and THROUGHPUT that form the basis of the economic performance criteria (Section 1.2). Therefore, the rest of the simulation will focus on the first 250 minutes to ensure that the disturbance rejection capabilities of the various controllers are clear with regard to PSE, LOAD, SLEV and THROUGHPUT.

5.3.2 Constant setpoint following and disturbance rejection

The most common operational mode for a milling circuit controller is to track a constant setpoint while rejecting external disturbances. The disturbances on the milling circuit can be quite severe, because the feed ore forms part of the grinding medium. Any changes to the size distribution or hardness of the ore will affect the throughput and grind of the milling circuit.

In this section the ability of the RNMPC, NMPC (shown in Section 3.7) and single-loop PI controllers (shown in Section 4.5) to follow constant setpoints of 80% $< 75\ \mu$m for PSE and 45% for mill load volume (LOAD) in the face of disturbances is examined. LOAD is controlled strictly to prevent underload and overload conditions in the mill. The underload condition can result in steel balls and rocks hitting the liners of the mill directly, severely increasing the wear of the liners. Overload and underload conditions cause a drop in milling efficiency and affect the grind.

The simulation results illustrated in Figure 5.4a, Figure 5.5a, Figure 5.4b and Figure 5.5b show the RNMPC tracking the constant setpoints on PSE and LOAD without any step disturbances. Zero mean parameter variations are, however, present as summarised in Table 5.2. The simulation results for NMPC are discussed in Section B.1.1.

The simulation scenario shown in Figure 5.4a and Figure 5.5a allows SLEV to vary freely with only upper and lower constraints enforced. Steering SLEV to setpoint compared to allowing SLEV to vary freely does not significantly influence the closed-loop performance under RNMPC in terms of PSE setpoint tracking and the average circuit throughput (Table 5.4). Allowing SLEV to vary within bounds allows the RNMPC to change the density of the slurry inside the sump (assuming fully mixed conditions) and as a result allows the RNMPC to control the feed density to the cyclone. Control of the feed density to the cyclone can increase the control envelope of the RNMPC.

The results of the milling circuit under PI control are illustrated in Figure 5.4c and Fig-

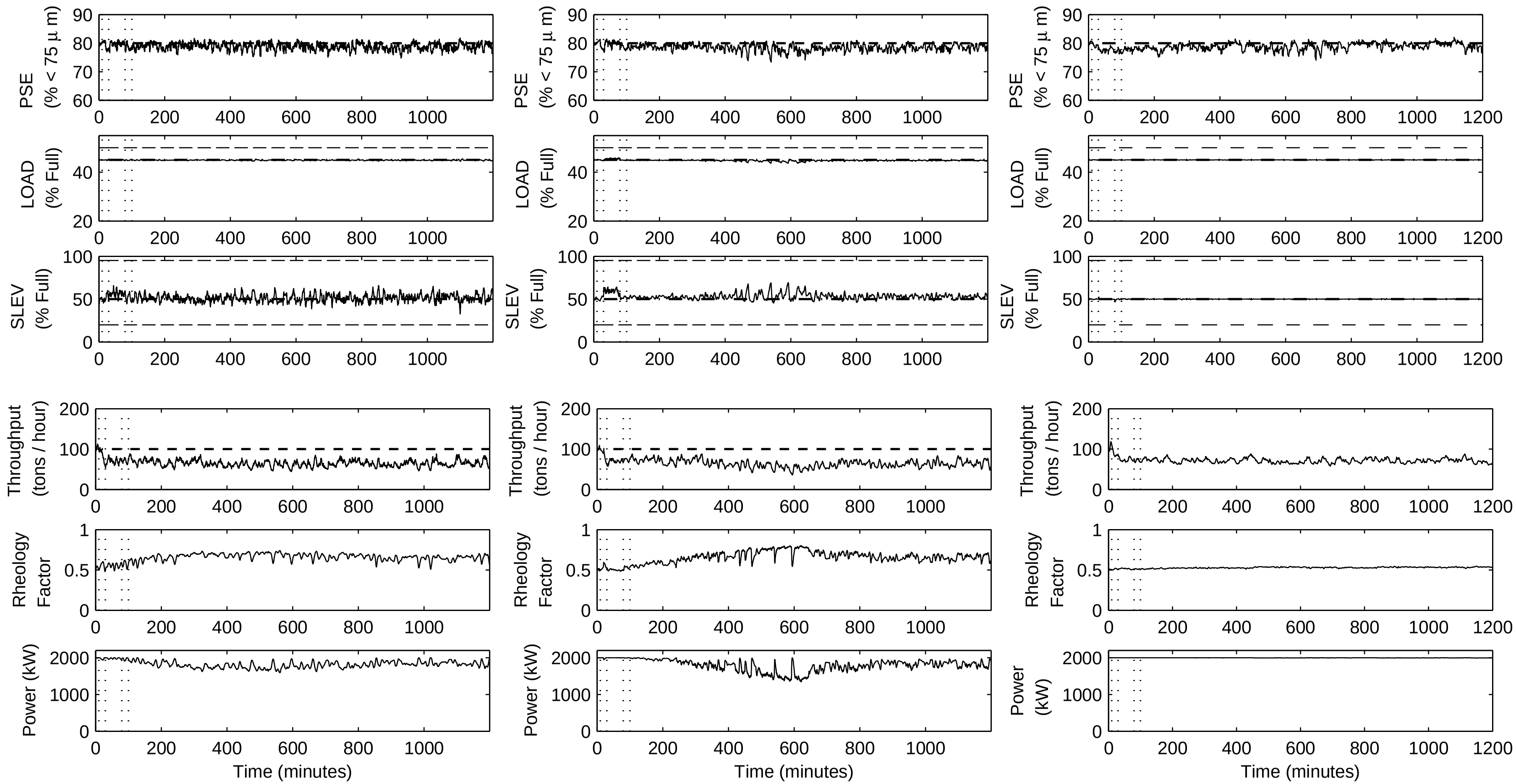

(a) RNMPC (b) NMPC (c) PI controllers.

Figure 5.2: CVs of RNMPC (a), NMPC (b) and PI controllers (c).
Feed ore hardness and composition step disturbances are present as well as a sump feed water disturbance simulating spillage water being added to the sump. This simulation is performed for 1200 minutes to determine the time to steady state. The dashed lines indicate the constraints on the variable and the vertical dotted lines indicate the start of the disturbance events. The dash-dot line indicates the setpoint.

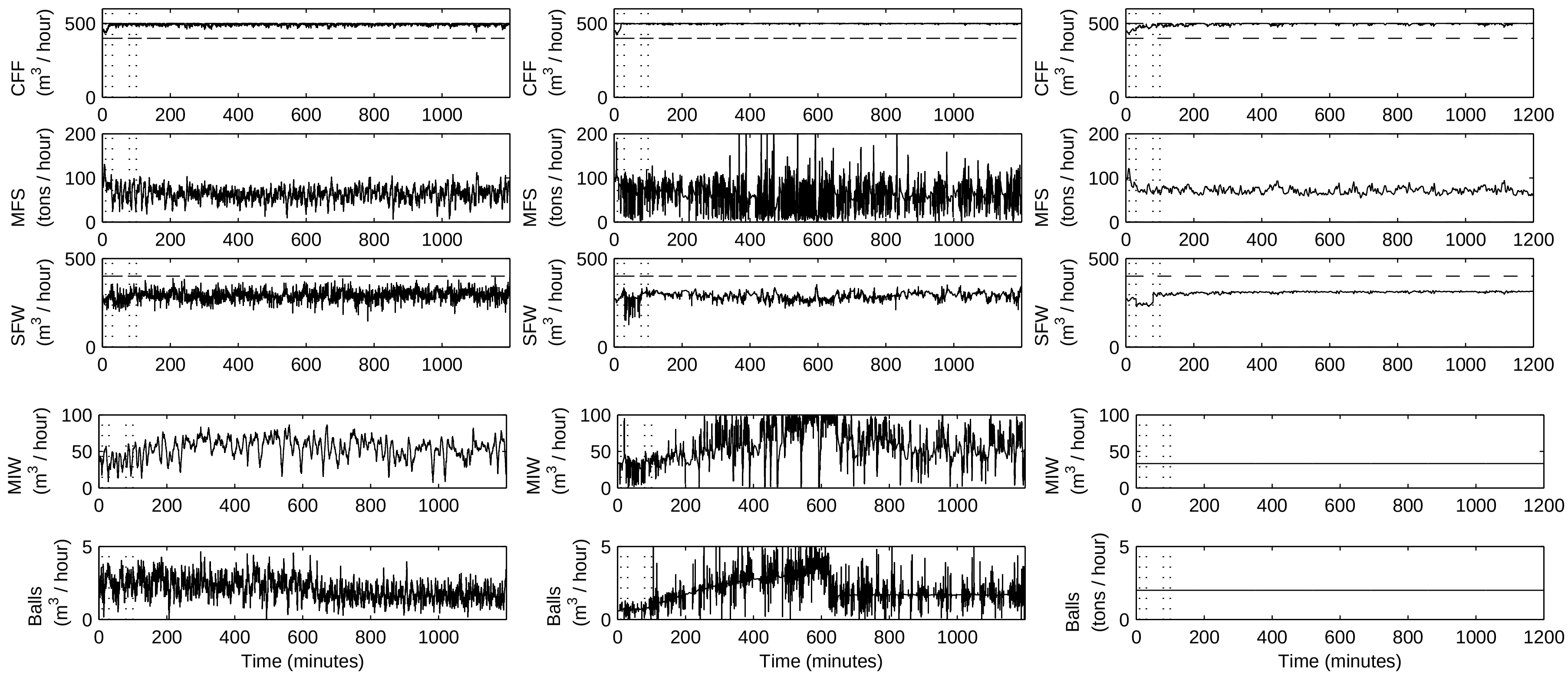

(a) RNMPC (b) NMPC (c) PI controllers.

Figure 5.3: MVs of RNMPC (a), NMPC (b) and PI controllers (c).
Feed ore hardness and composition step disturbances are present as well as a sump feed water disturbance simulating spillage water being added to the sump. This simulation is performed for 1200 minutes to determine the time to steady state. The dashed lines indicate the constraints on the variable and the vertical dotted lines indicate the start of the disturbance events. The dash-dot line indicates the setpoint.

ure 5.5c. Table 5.4 shows that the PSE tracking of the PI controllers is not as tight as the RNMPC at a comparable average throughput.

Other simulations investigating the effects of various disturbances will be compared against the baseline simulations presented in Figure 5.4 and Figure 5.5.

A 50% increase in feed ore hardness is introduced at time 180 minutes. The RNMPC (Figure 5.6a and Figure 5.7a) and NMPC (Figure 5.6b and Figure 5.7b) follow the PSE and LOAD setpoints very tightly despite the increase in feed ore hardness, as seen in Table 5.4. The PI controllers (Figure 5.6c and Figure 5.7c), however, show a drop in PSE when the ore hardness disturbance is introduced and this is reflected in a higher PSE error, as seen in Table 5.4.

The controller decreases MFS, causing the average throughput of the milling circuit to decrease as the ore hardness increases, because the harder ore needs more time inside the mill to grind down. The controller does not decrease MFS enough to maintain the grind of the mill, which causes the ratio of coarse to fine material in the sump to increase. The controller increases the CFF to compensate for the coarser grind in order to maintain PSE at setpoint, because higher pressure at the inlet of the cyclone results in finer material exiting at the overflow of the cyclone, called a finer cut, while lower pressure at the cyclone inlet results in a coarser cut. The cyclone feed contains more coarse material and a finer cut is therefore required to maintain PSE at setpoint. The increase in CFF also causes an increase in the recirculating load of the circuit due to the coarser grind of the mill. The controller allows the grind to become coarser and then compensates by increasing CFF in order to minimise the impact of the harder ore on the throughput while maintaining PSE at setpoint.

The amount of rocks in the feed ore is increased by 50% at time 180 minutes to simulate a feed disturbance. The RNMPC (Figure 5.8a and Figure 5.9a) and NMPC (Figure 5.8b and Figure 5.9b) follow the PSE and LOAD setpoints very tightly despite the increase of rocks in the feed ore as seen in Table 5.4. The PI controllers (Figure 5.8c and Figure 5.9c), however, show a slight increase in PSE as the increased amount of rocks inside the mill results in a finer grind. There is no immediate impact on the performance of the mill, but there is a build-up of rocks inside the mill that will eventually result in a decrease in throughput, because it takes longer to grind down the rocks inside the mill. Figure 5.10 and Figure 5.11 show the result of the milling circuit under RNMPC (a), NMPC (b) and PI control (c) when the feed disturbance is introduced at time 10 minutes. The build-up of rocks inside the mill produces more fines and forces the controller to decrease CFF in order to maintain PSE.

A 50 $\mathrm{m}^3/\mathrm{hour}$ increase in SFW is introduced at time 180 minutes to simulate spillage pumping. The RNMPC (Figures 5.12a and Figure 5.13a) follows the PSE and LOAD setpoints more tightly compared to the NMPC (Figures 5.12b and Figure 5.13b) and PI controller (Figures 5.12c and Figure 5.13c), as seen in Table 5.4, but SLEV increases slightly under both RNMPC and NMPC owing to the disturbance. The sump is assumed to be fully mixed and the increase in water lowers the slurry density inside the sump, resulting in a finer cut at the cyclone overflow, which forces the controller to reduce CFF in order to maintain PSE at its setpoint.

In this scenario the feed ore hardness increases at time 10 minutes, SFW increases between 30 minutes and 80 minutes and the percentage of rocks in the feed increases at time 100 minutes. These disturbances are present in all subsequent simulations. The RNMPC (Figure 5.14a and Figure 5.15a) and NMPC (Figure 5.14b and Figure 5.15b) follow the PSE and LOAD setpoints very tightly despite all the disturbance working on the system. The PI controllers (Figure 5.14c and Figure 5.15c), however, show a larger PSE tracking error compared to the RNMPC and NMPC with all the disturbances present. Comparing Figure 5.15a and Figure 5.15b, it is clear that the NMPC is more aggressive in its control action compared to the RNMPC. The RNMPC follows the PSE setpoint more closely than the NMPC, as seen in Table 5.4. Figure 5.14 shows that all the controllers operate at the upper constraint of CFF, which suggests that the RNMPC and NMPC controllers use other variables in conjunction with CFF to maintain PSE at its setpoint.

5.3.3 Reduced PSE setpoint to 75% and 70% $< 75\mu$m

The increased hardness of the feed ore caused the average throughput of the circuit to reduce, because the ore needs more time to grind down. There is a well-established inverse relationship between PSE and throughput (Craig and MacLeod, 1995). The PSE setpoint is reduced in order to increase the milling circuit throughput. The simulations in this scenario investigate what effect a reduction of 5% and 10% in PSE setpoint has on the average throughput of the system.

Figure 5.16b and Figure 5.17b show that the RNMPC tracks the reduced PSE setpoint of 75% $< 75\mu$m and LOAD setpoint of 45% volumetric filling well. The throughput shows large variations due primarily to the ore hardness and composition variations. Decreasing the setpoint for PSE to 75% increased the average throughput of the milling circuit to 74.5 from 72.2 tons per hour. The PI controllers (Figure 5.18b and Figure 5.19b) show significantly better tracking of the PSE setpoint as well as increased throughput. The improved PSE tracking can primarily be attributed to the controller maintaining CFF within its constraints, because CFF is the only manipulated variable available to the PI controllers for controlling PSE.

Figure 5.16c and Figure 5.17c show that the RNMPC tracks the reduced PSE setpoint of 70% $< 75\mu$m and LOAD setpoint well. Decreasing the PSE setpoint to 70% resulted in an average throughput of 81.3 tons per hour, as seen in Table 5.4. The ability of the PI controllers (Figure 5.18c and Figure 5.19c) to track the PSE setpoint of 70% compared to 75% is significantly poorer. The poorer PSE tracking can primarily be attributed to CFF operating at its lower limit and reducing the ability of the PI controllers to control PSE.

Decreasing the PSE setpoint by 10% could not compensate for the 50% increase in ore hardness. Maintaining the throughput at 100 tons per hour would probably require the PSE setpoint to be lowered to an unacceptably low value. The corresponding results for NMPC are discussed in Section B.1.2.

5.3.4 Step change of -5% and -10% in PSE setpoint

Changes in setpoints occur as the result of changing production targets and changing milling conditions. In the previous section, the increased ore hardness required that the PSE setpoint be reduced in order to maintain the circuit throughput at the desired level. In this section, the ability of the controller to track a modest and large setpoint change in PSE is investigated.

A -5% step change in PSE setpoint is introduced at time 100 minutes, while maintaining a constant setpoint on LOAD and SLEV. The RNMPC (Figure 5.20a and Figure 5.21a) and NMPC (Figure 5.20b and Figure 5.21b) follow the setpoint change well without affecting LOAD. The decrease in particle size setpoint increased throughput by a small margin from 72.2 to 74.0 tons per hour. The PI controllers (Figure 5.20c and Figure 5.21c) start to drift below the PSE setpoint but track the reduced setpoint after the step change very well, because the controller can maintain CFF within its limits.

A larger step change of -10% in the PSE setpoint is introduced at time 100 minutes, while maintaining a constant setpoint on LOAD and SLEV. The RNMPC (Figure 5.20a and Figure 5.21a) and NMPC (Figure 5.20b and Figure 5.21b) follow the larger setpoint change well without affecting LOAD. The decrease in PSE setpoint increased throughput by a bigger margin from 72.2 to 76.7 tons per hour. The PI controllers (Figure 5.20c and Figure 5.21c) start to drift below the PSE setpoint when the ore hardness disturbance is introduced. The PI controllers cannot follow the lower PSE after the setpoint step change, because CFF reaches its lower limit, reducing the ability of the PI controllers to control PSE. The RNMPC and NMPC increase the mill rheology by primarily increasing MIW, which will reduce the density of the slurry in the sump as well as the grinding efficiency of the mill, resulting in a decrease in PSE while CFF is constrained at its lower limit.

The RNMPC, NMPC and PI controllers showed a decoupled response by successfully changing PSE without any significant impact on LOAD and SLEV. The PI controllers were not able to handle the big PSE setpoint change as well as the RNMPC and NMPC controllers, because the PI controllers can only use CFF to control PSE, while the RNMPC and NMPC can use other variables, such as MIW and SFW, to control PSE.

5.3.5 Regulate PSE, LOAD and Throughput

The previous two sections show the dependence of throughput on PSE and ore hardness. Throughput is added to the objective function of the controller in order to determine if the optimising capability of the controller can be exploited to increase the average throughput of the circuit while maintaining PSE at the desired setpoint when the ore hardness increases.

Figure 5.24b and Figure 5.25b show that adding the throughput to the objective function causes the RNMPC to make a trade-off between following the PSE setpoint and throughput setpoint according to their respective weightings. Table 5.4 shows that the PSE error increases significantly and that the average throughput decreases from 72.2 to 70.8 tons per hour, resulting in an overall worst result. Figure 5.25b shows large variation in the manipulated variables that can be the cause of the poor overall performance.

Figure 5.24c and Figure 5.25c show that increasing the throughput weighting causes a larger error in the PSE tracking performance while further reducing the average throughput as seen in Table 5.4.

The unexpected reduction in throughput can be attributed to the large variations in the manipulated variables as observed in Figure 5.25c. The large variations may be the result of the gain of the controller being too high. The gain of the controller is controlled by the weighting on the manipulated and controlled variables and more importantly the ratio of the weights between the controlled and manipulated variables. The contribution of the controlled variables to the objective function compared to the manipulated variables is increased by adding throughput to the objective function, effectively reducing the weighting of the manipulated variables and increasing the gain of the controller.

Figure 5.26c and Figure 5.27c show that oscillations are eliminated from the control action by increasing the weighting on the manipulated variables. The PSE tracking error is reduced and the average throughput increased compared to the scenario shown in Figure 5.24b and Figure 5.25b. The PSE tracking is worse but the average throughput is higher than the case where throughput is not included in the performance function (Figure 5.14a and Figure 5.15a), as seen in Table 5.4.

The results in this section show that the controller cannot overcome the inherent trade-off between PSE and throughput, because the controller lowers PSE in order to increase throughput. The corresponding results for NMPC are discussed in Section B.1.3.

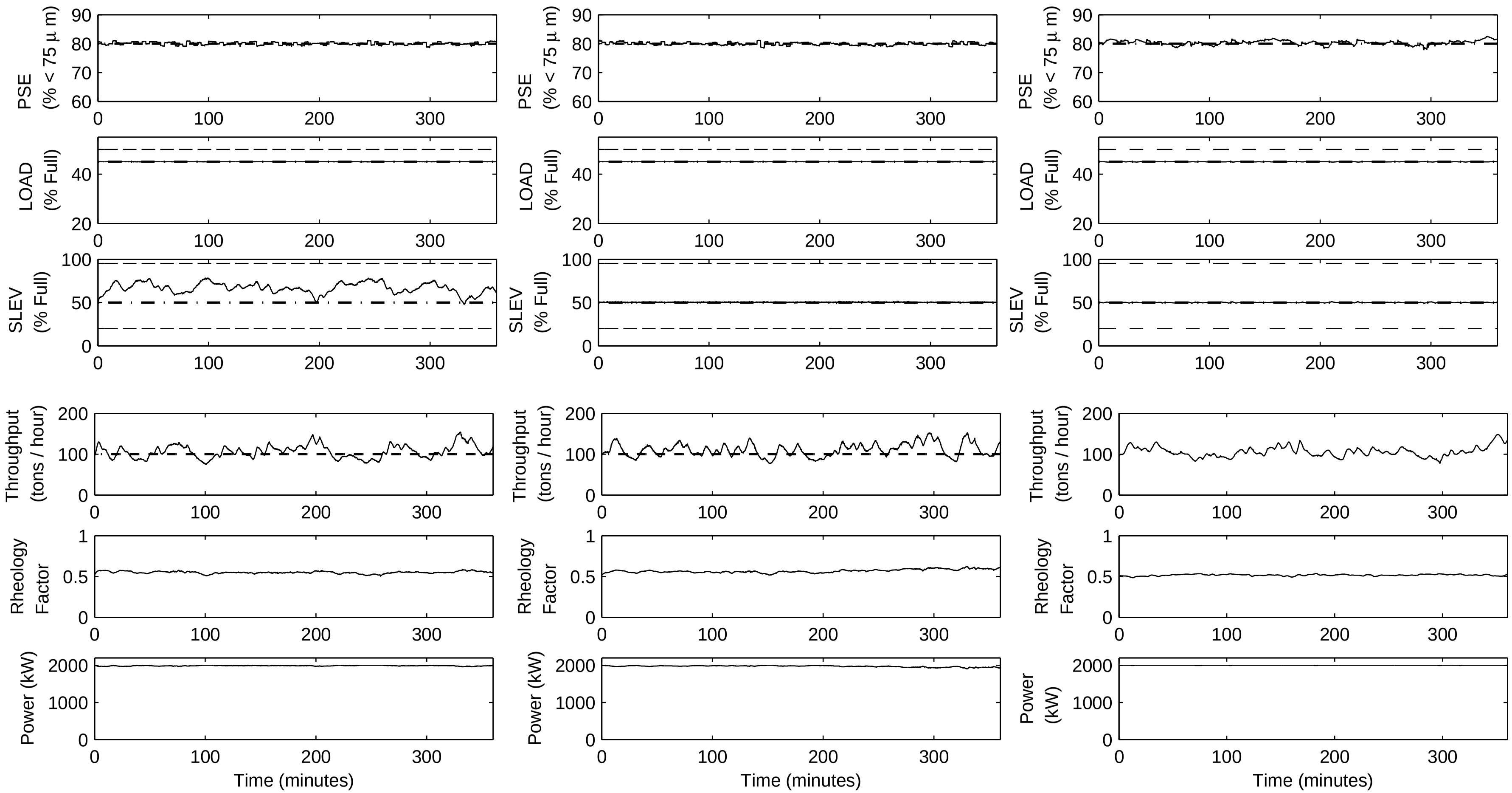

(a) RNMPC without SLEV weighting. (b) RNMPC with SLEV weighting. (c) PI controllers.

Figure 5.4: CVs of RNMPC (a) & (b) and PI controllers (c).
There is no step disturbance present in either the feed ore hardness or the fraction of rocks in the feed ore. This represents the nominal scenario with only zero mean parameter variations present. The dashed lines indicate the constraints on the variable and the vertical dotted lines indicate the start of the disturbance events. The dash-dot line indicates the setpoint.

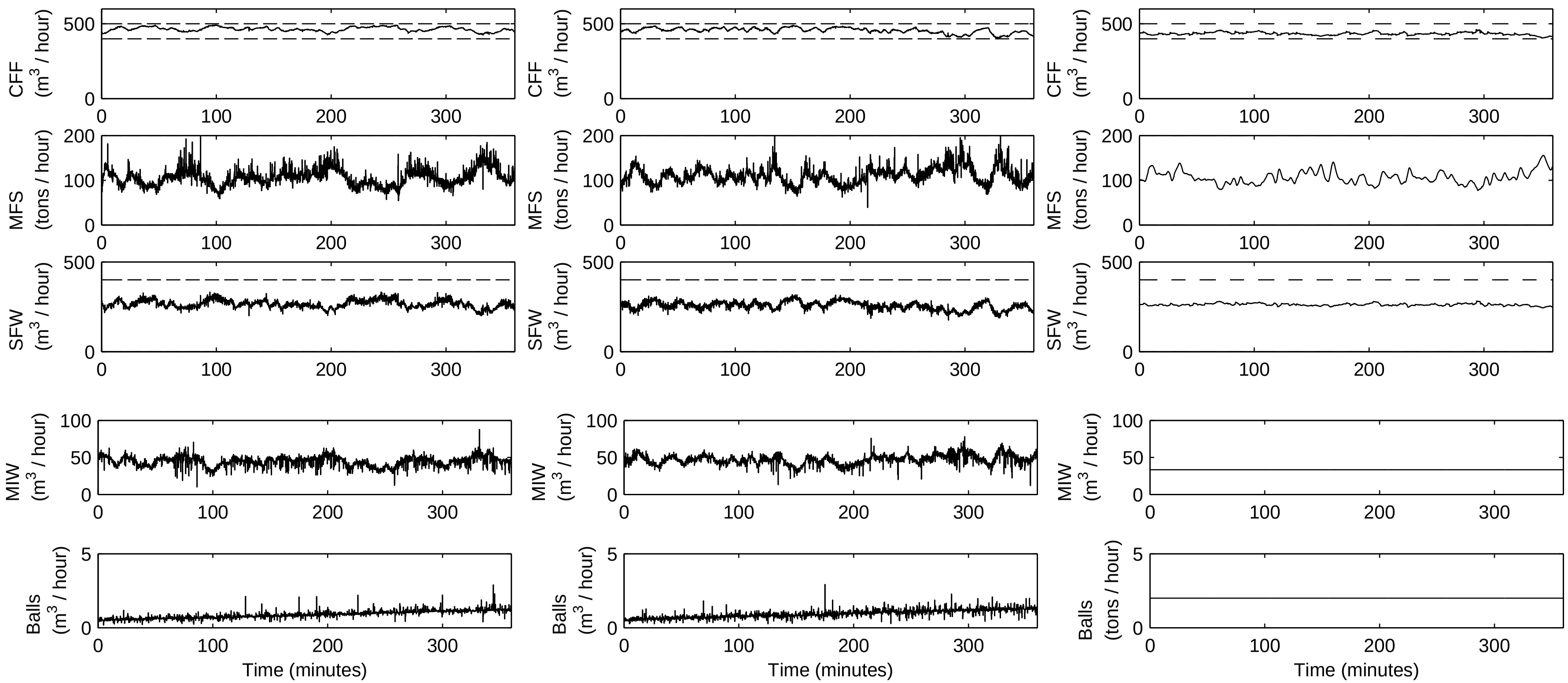

(a) RNMPC without SLEV weighting.

(b) RNMPC with SLEV weighting.

(c) PI controllers.

Figure 5.5: MVs of RNMPC (a) & (b) and PI controllers (c).
There is no step disturbance present in either the feed ore hardness or the fraction of rocks in the feed ore. This represents the nominal scenario with only zero mean parameter variations present. The dashed lines indicate the constraints on the variable and the vertical dotted lines indicate the start of the disturbance events. The dash-dot line indicates the setpoint.

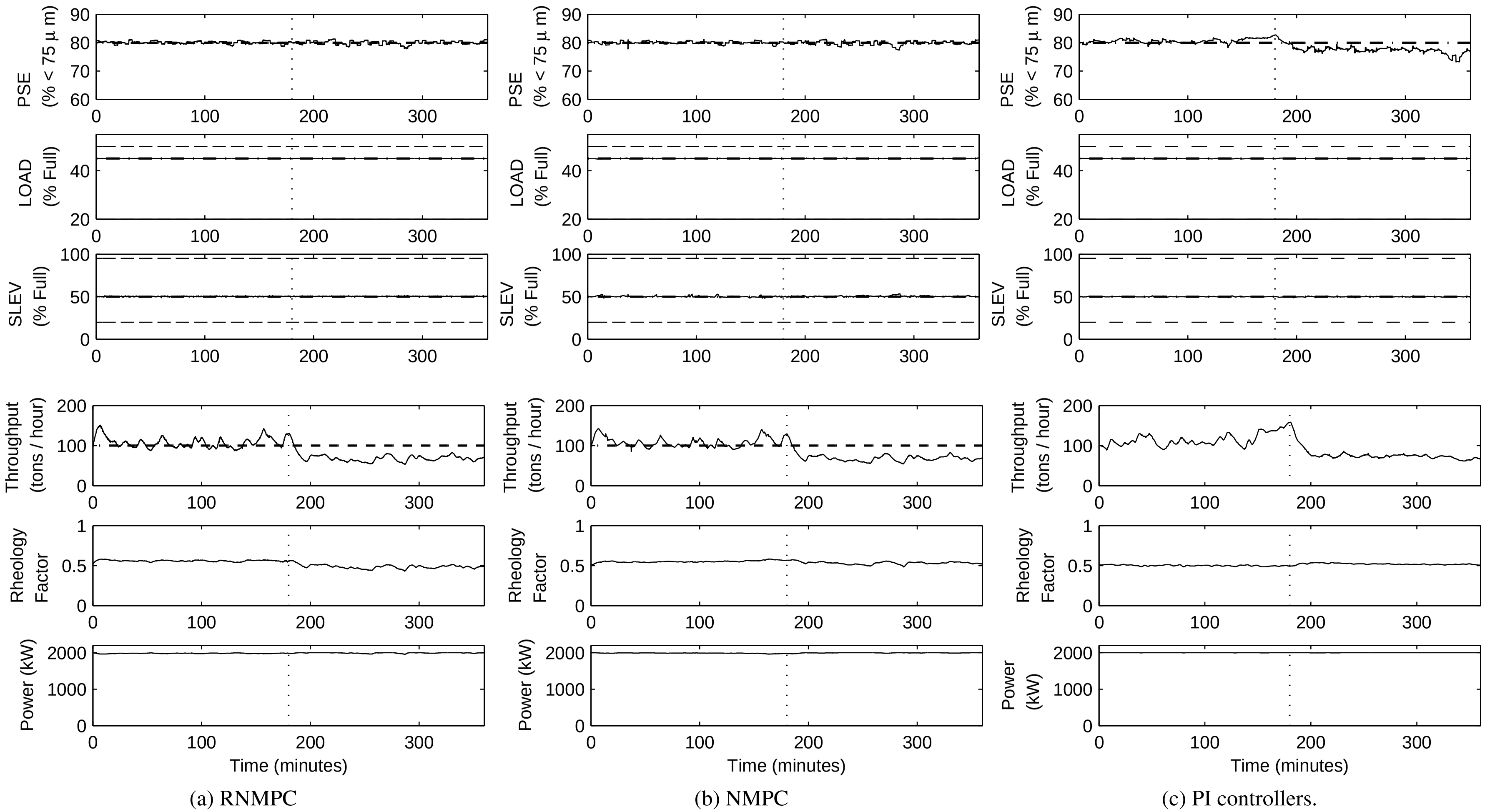

(a) RNMPC (b) NMPC (c) PI controllers.

Figure 5.6: CVs RNMPC (a), NMPC (b) and PI (c) controllers.
A 50% increase in ore hardness is introduced at time 180 minutes. The dashed lines indicate the constraints on the variable and the vertical dotted lines indicate the start of the disturbance events. The dash-dot line indicates the setpoint.

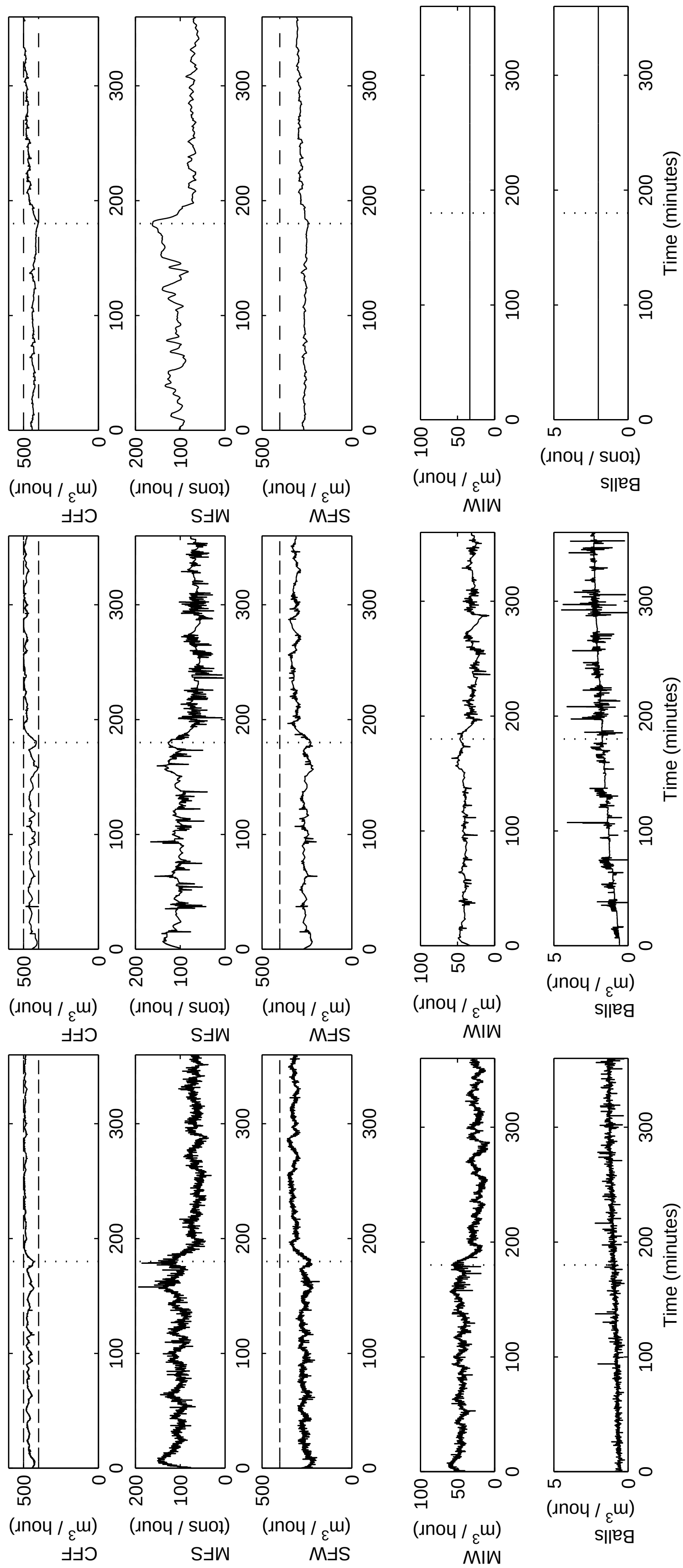

(a) RNMPC (b) NMPC (c) PI controllers.

Figure 5.7: MVs RNMPC (a), NMPC (b) and PI (c) controllers.
A 50% increase in ore hardness is introduced at time 180 minutes. The dashed lines indicate the constraints on the variable and the vertical dotted lines indicate the start of the disturbance events. The dash-dot line indicates the setpoint.

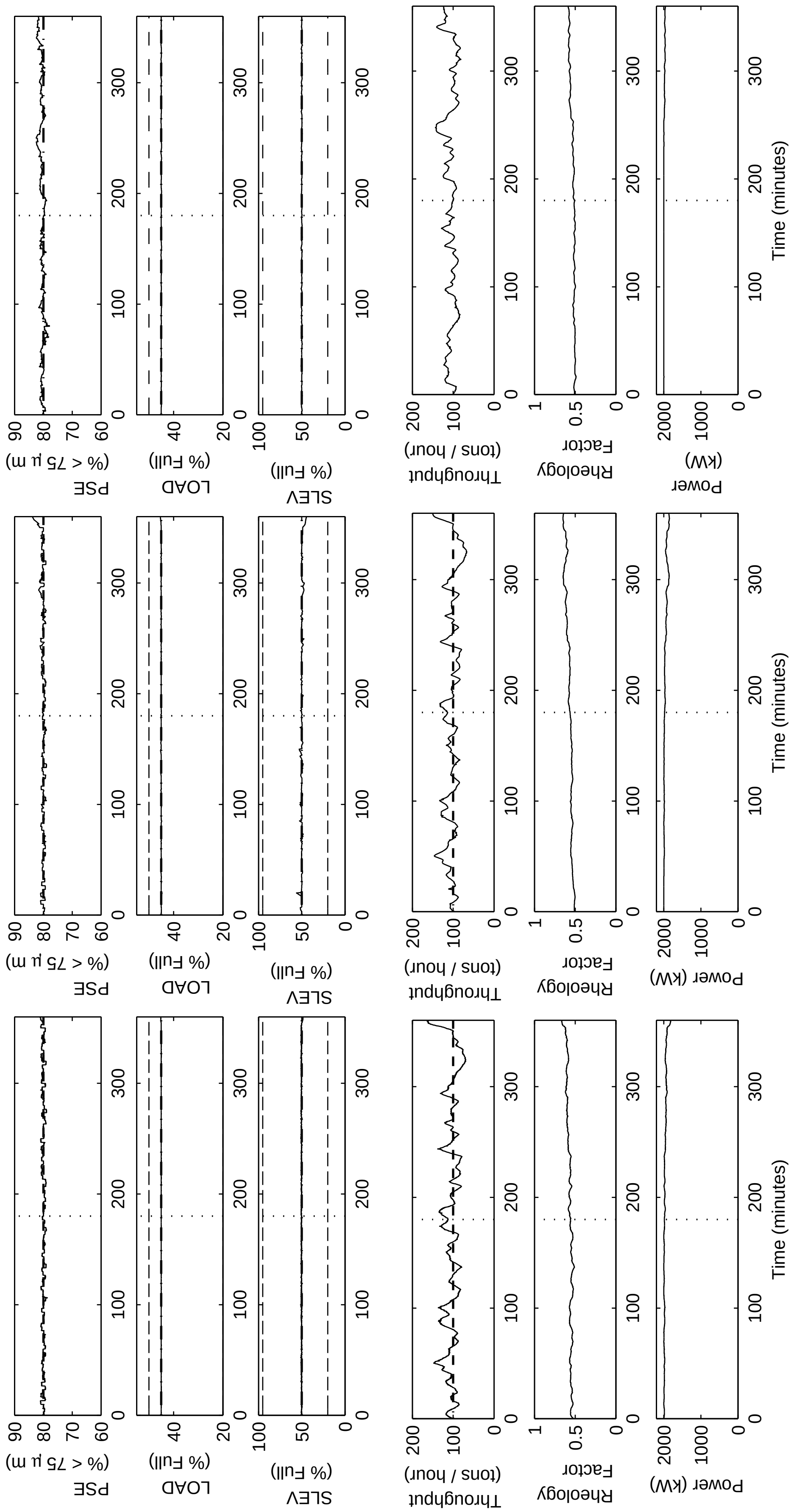

Figure 5.8: CVs RNMPC (a), NMPC (b) and PI (c) controllers.
A 50% increase in the fraction of rocks in the feed ore is introduced at time 180 minutes. The dashed lines indicate the constraints on the variable and the vertical dotted lines indicate the start of the disturbance events. The dash-dot line indicates the setpoint.

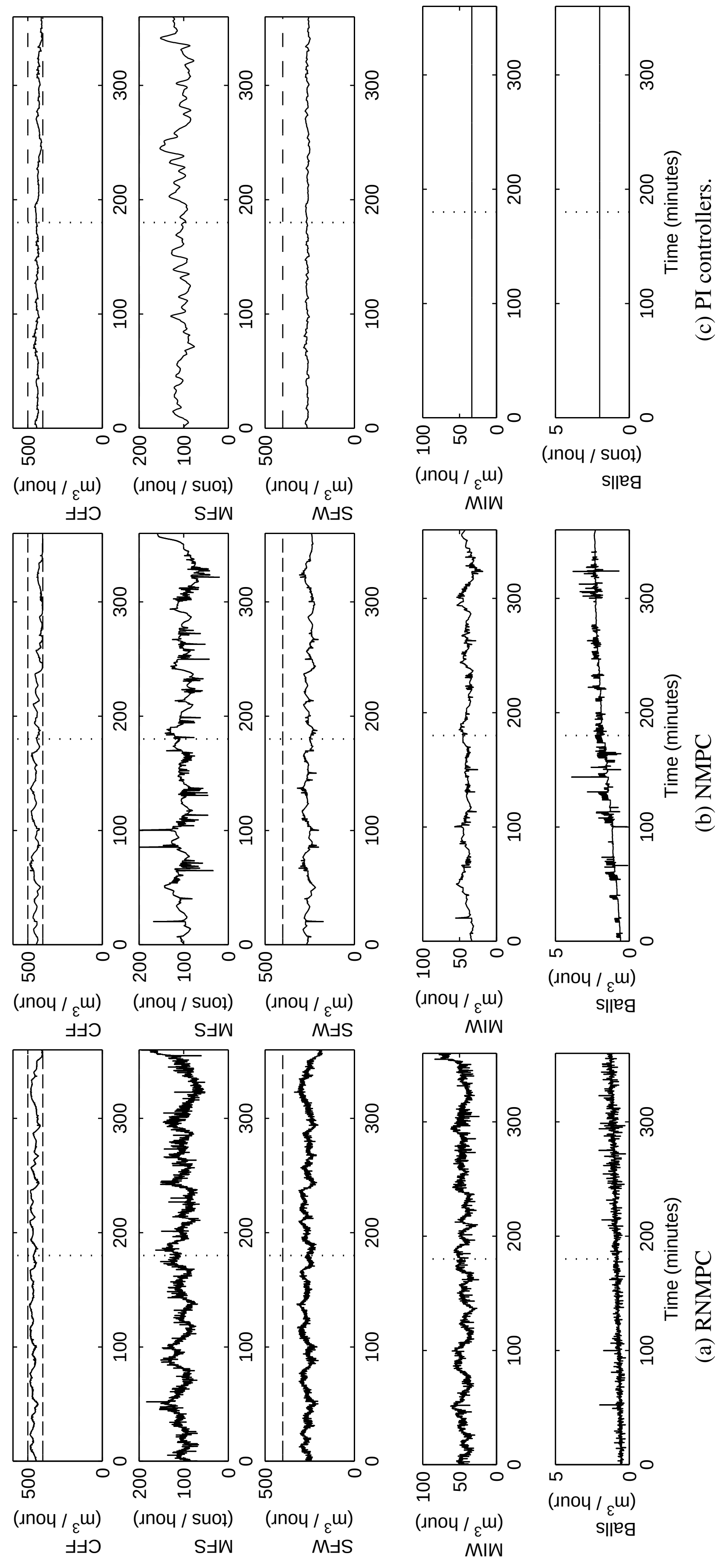

Figure 5.9: MVs RNMPC (a), NMPC (b) and PI (c) controllers.
A 50% increase in the fraction of rocks in the feed ore is introduced at time 180 minutes. The dashed lines indicate the constraints on the variable and the vertical dotted lines indicate the start of the disturbance events. The dash-dot line indicates the setpoint.

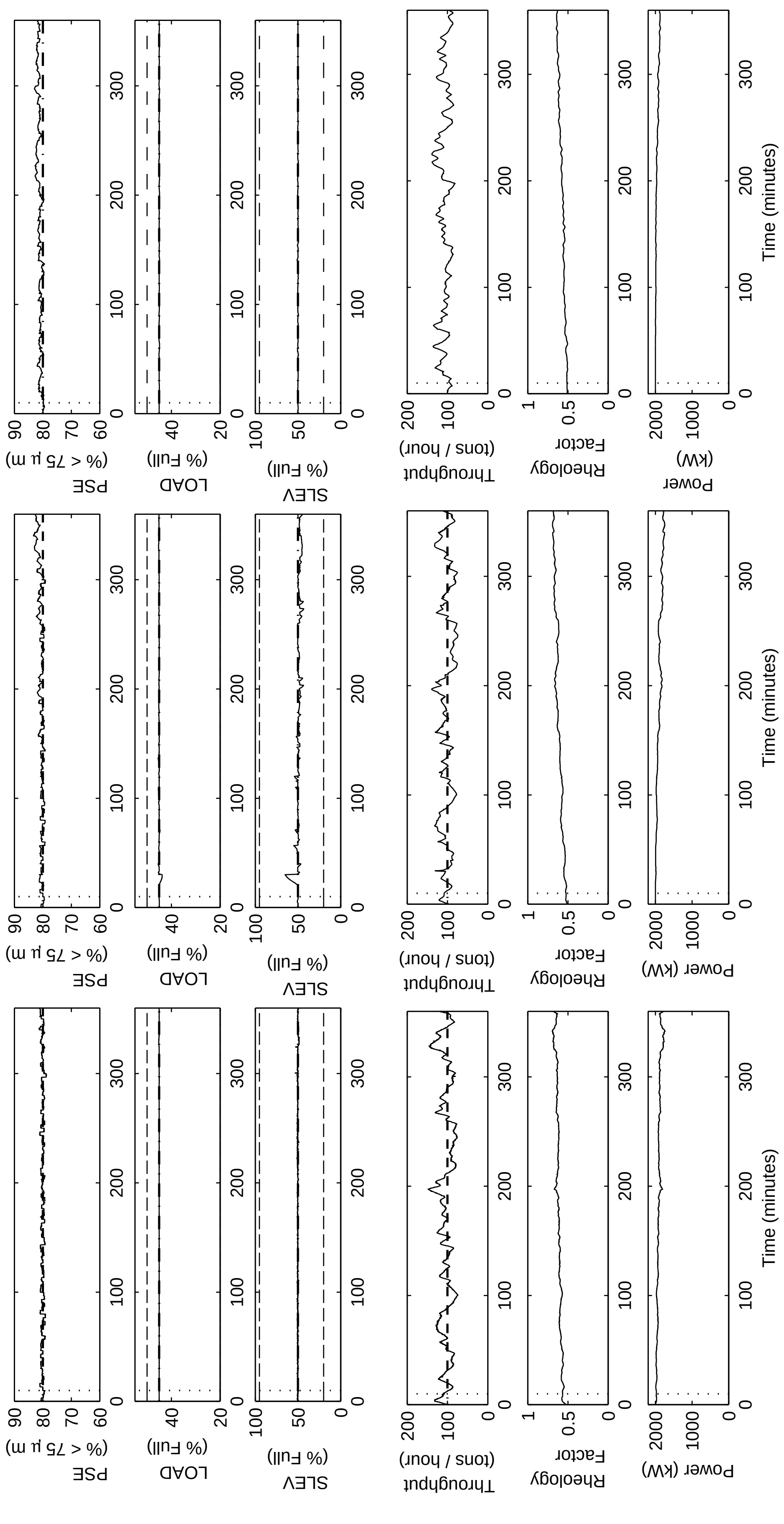

(a) RNMPC

(b) NMPC

(c) PI controllers.

Figure 5.10: CVs RNMPC (a), NMPC (b) and PI (c) controllers. A 50% increase in the fraction of rocks in the feed ore is introduced at time 10 minutes. The dashed lines indicate the constraints on the variable and the vertical dotted lines indicate the start of the disturbance events. The dash-dot line indicates the setpoint.

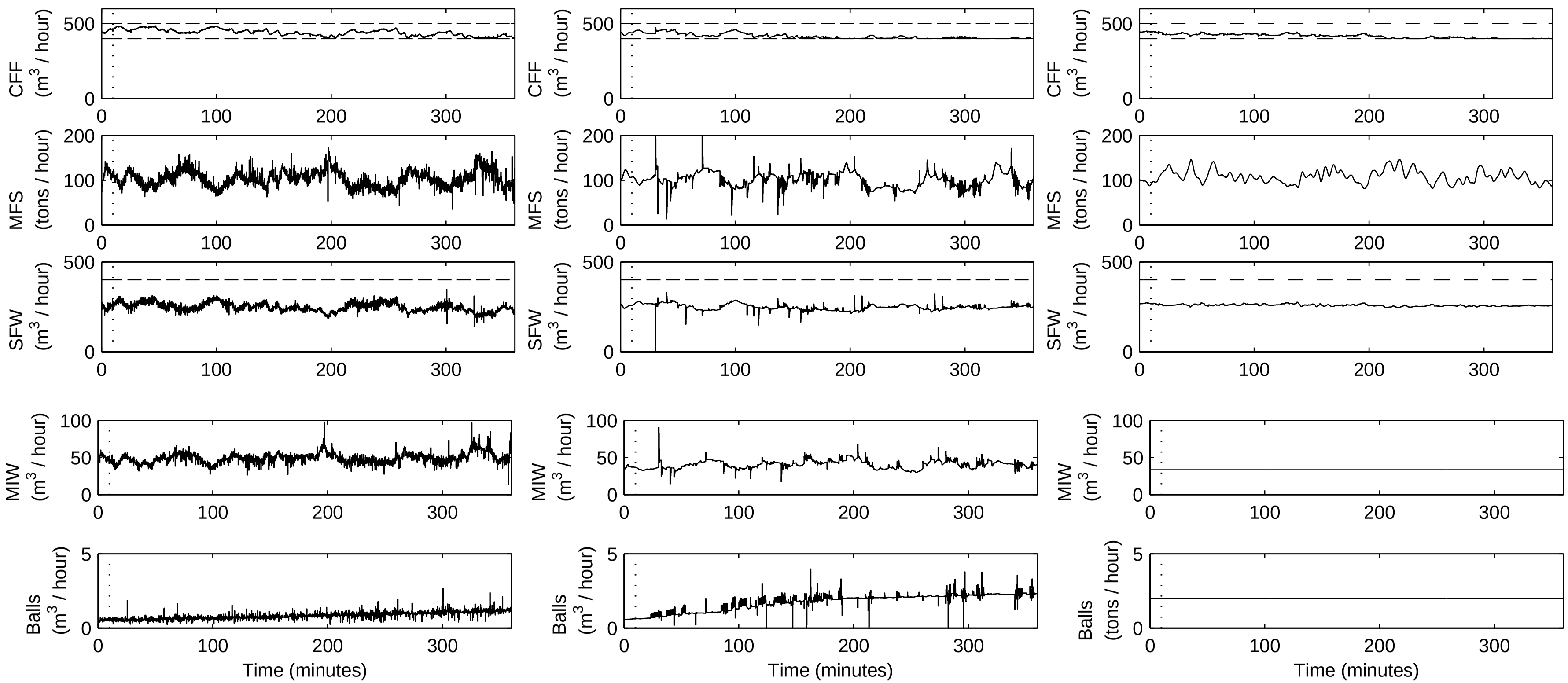

(a) RNMPC (b) NMPC (c) PI controllers.

Figure 5.11: MVs RNMPC (a), NMPC (b) and PI (c) controllers.
A 50% increase in the fraction of rocks in the feed ore is introduced at time 10 minutes. The dashed lines indicate the constraints on the variable and the vertical dotted lines indicate the start of the disturbance events. The dash-dot line indicates the setpoint.

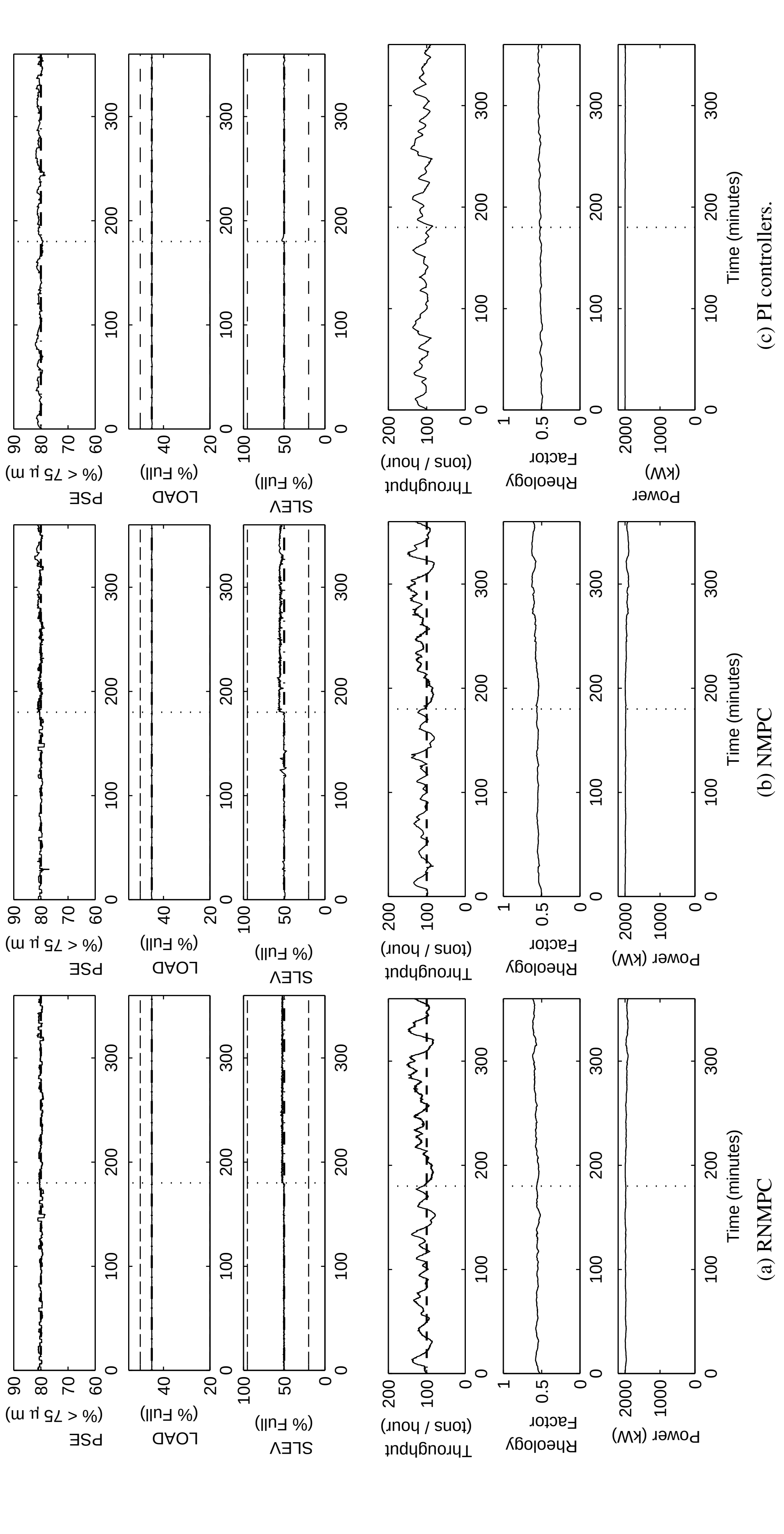

Figure 5.12: CVs RNMPC (a), NMPC (b) and PI (c) controllers. A 50 $m^3/_{hour}$ increase in SFW is introduced at time 180 minutes. The dashed lines indicate the constraints on the variable and the vertical dotted lines indicate the start of the disturbance events. The dash-dot line indicates the setpoint.

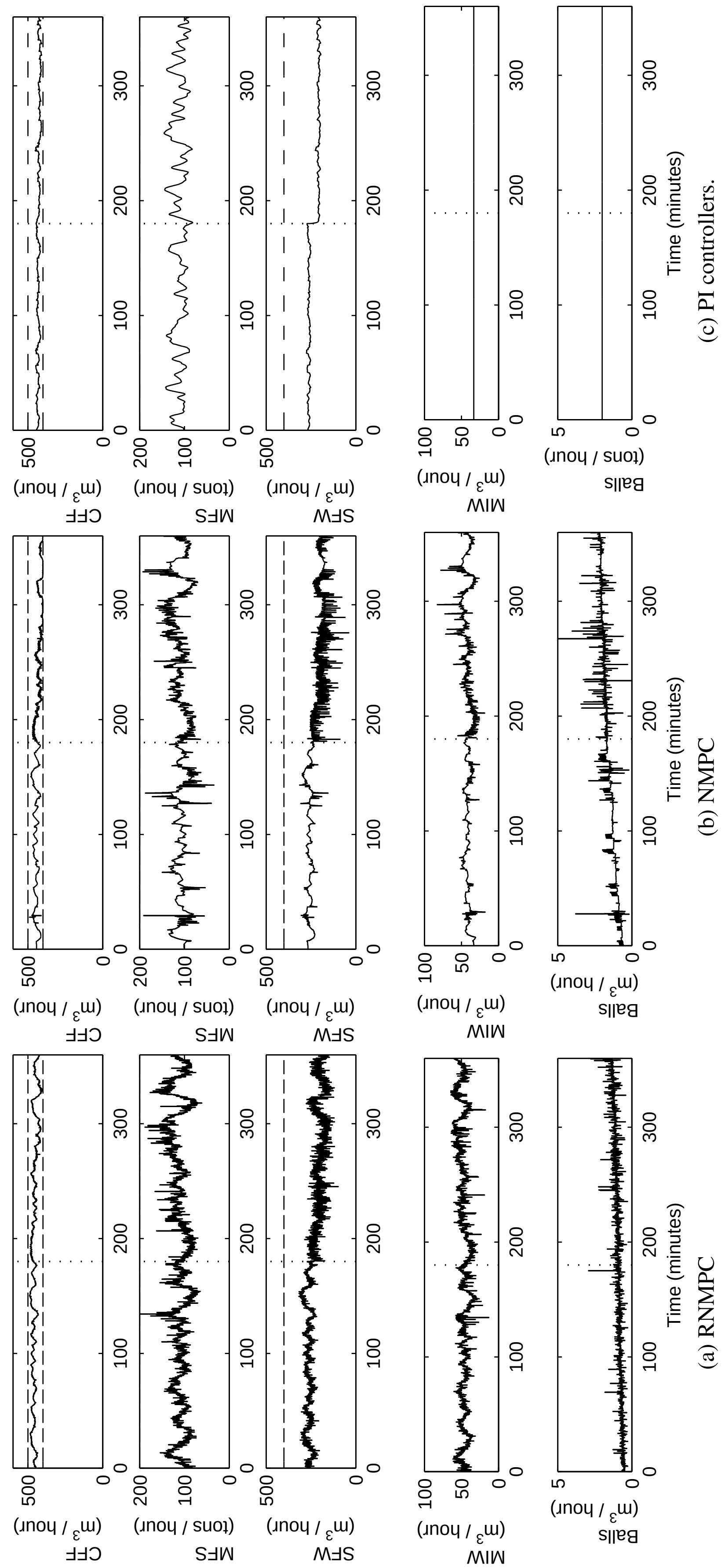

Figure 5.13: MVs RNMPC (a), NMPC (b) and PI (c) controllers. A 50 $m^3/_{hour}$ increase in SFW is introduced at time 180 minutes. The dashed lines indicate the constraints on the variable and the vertical dotted lines indicate the start of the disturbance events. The dash-dot line indicates the setpoint.

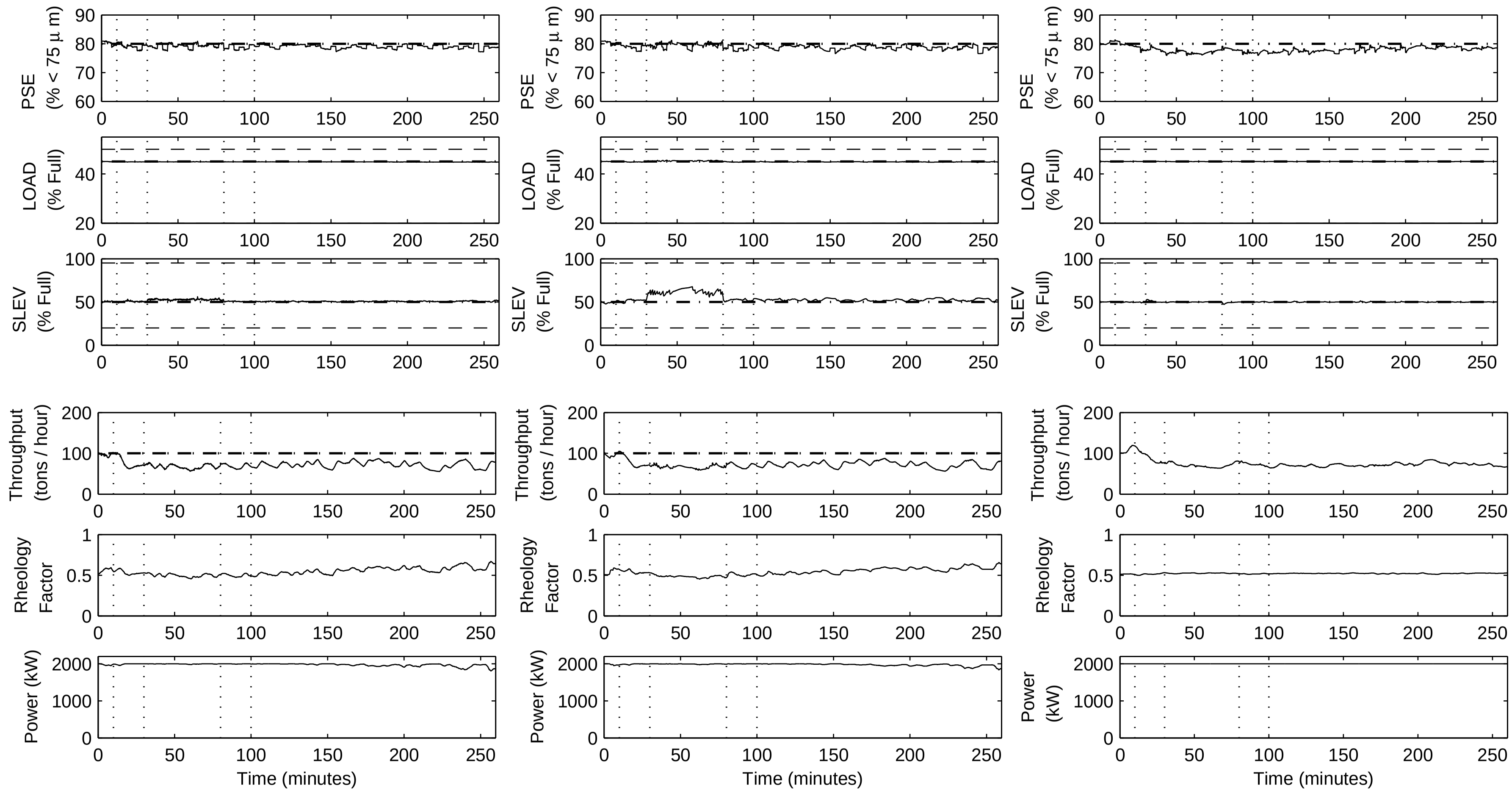

(a) RNMPC (b) NMPC (c) PI controllers.

Figure 5.14: CVs RNMPC (a), NMPC (b) and PI (c) controllers.
This represents the nominal disturbance scenario. The controller regulates PSE, LOAD and SLEV at constant setpoints with step disturbances: (1) 50% increase in rock hardness at time 10 minutes; (2) increase of 50 $^{m^3}/_{hour}$ in SFW from time 30 minutes until time 80 minutes; (3) 50% increase in the fraction of rocks in the feed ore at time 100 minutes. The dashed lines indicate the constraints on the variable and the vertical dotted lines indicate the start of the disturbance events. The dash-dot line indicates the setpoint.

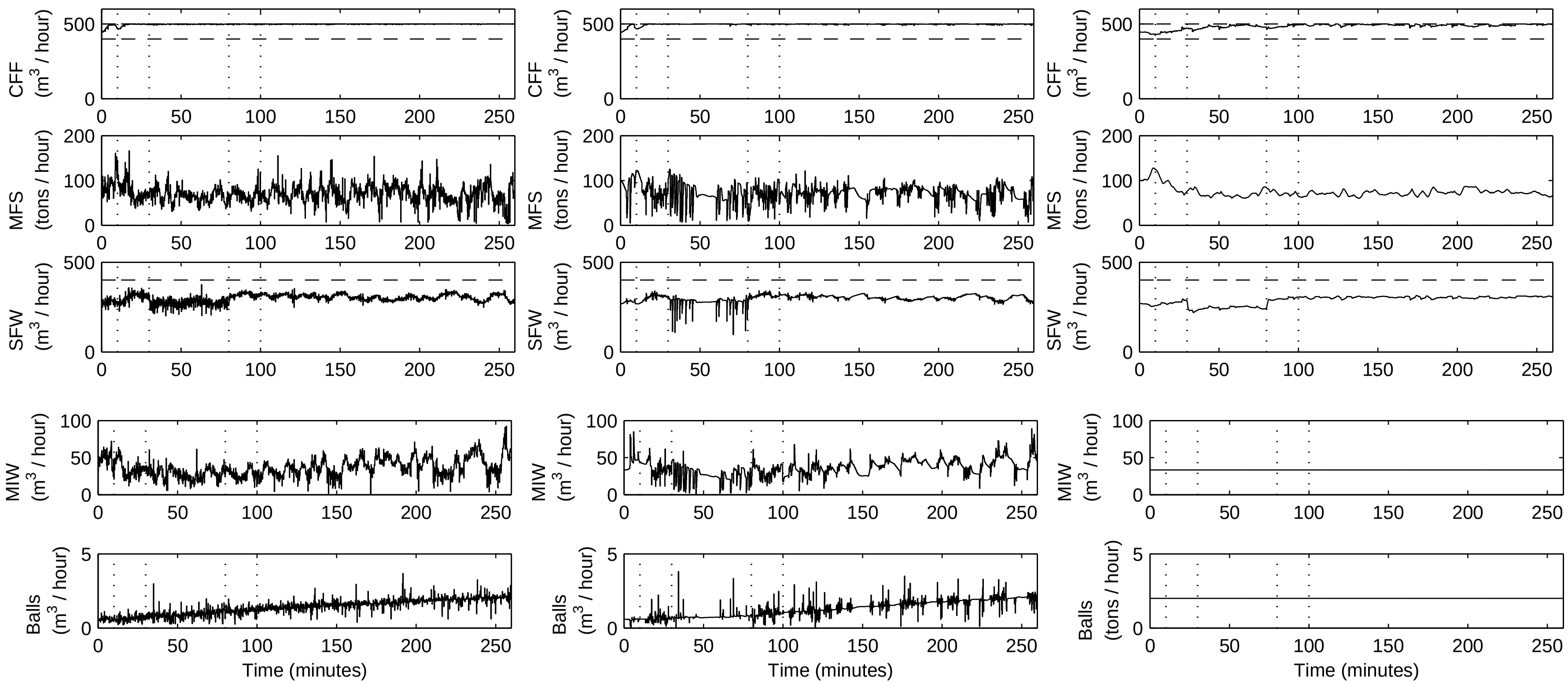

(a) RNMPC (b) NMPC (c) PI controllers.

Figure 5.15: MVs RNMPC (a), NMPC (b) and PI (c) controllers.
This represents the disturbance scenario. The controller regulates PSE, LOAD and SLEV at constant setpoints with step disturbances: (1) 50% increase in rock hardness at time 10 minutes; (2) increase of 50 $^{m^3}/_{hour}$ in SFW from time 30 minutes until time 80 minutes; (3) 50% increase in the fraction of rocks in the feed ore at time 100 minutes. The dashed lines indicate the constraints on the variable and the vertical dotted lines indicate the start of the disturbance events. The dash-dot line indicates the setpoint.

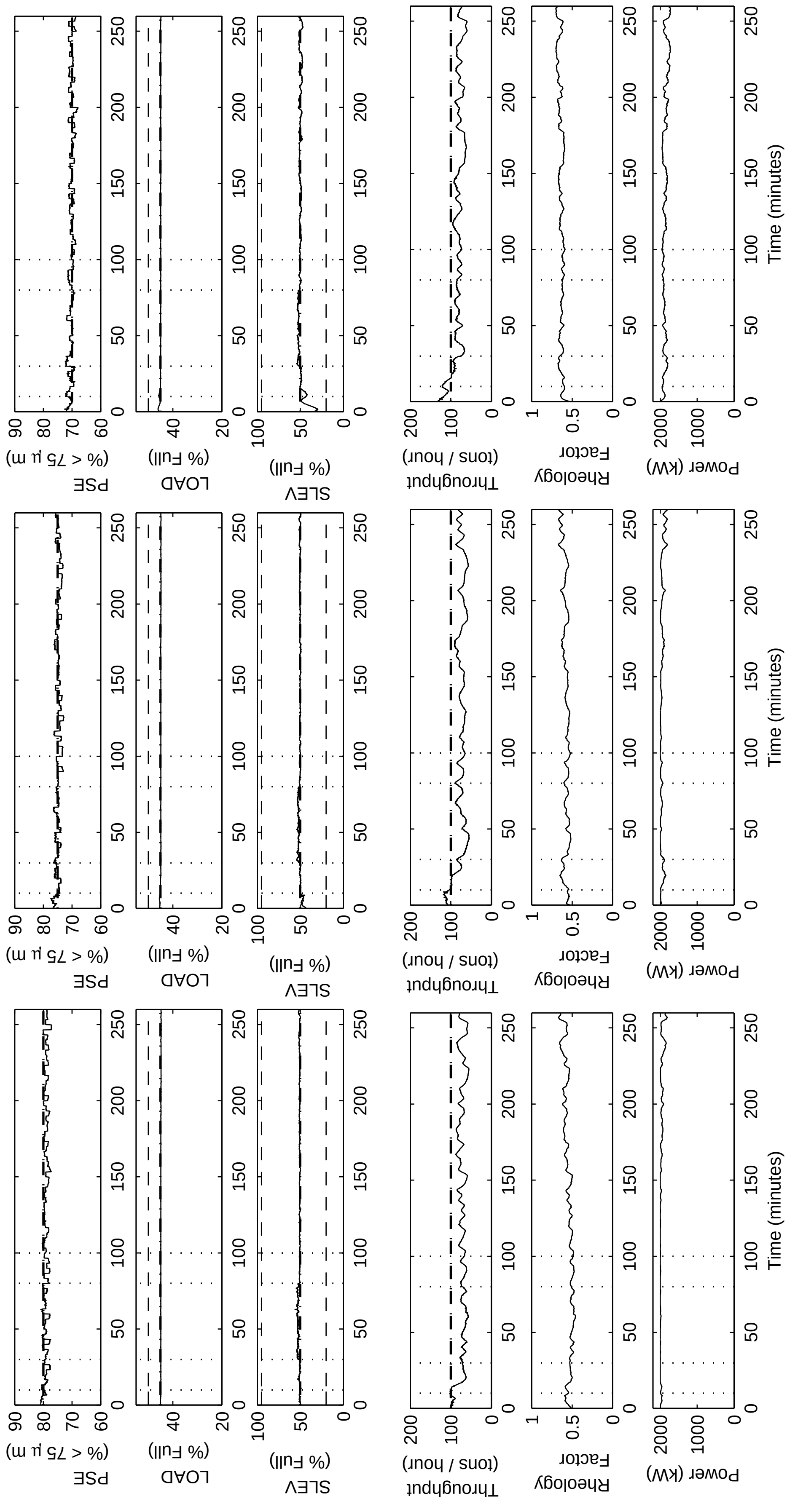

(a) PSE at 80. (b) PSE at 75. (c) PSE at 70.

Figure 5.16: CVs of the RNMPC.
The RNMPC regulates PSE at a constant setpoint of 80% (a), 75% (b) and 70% (c) with LOAD at a constant setpoint of 45% and SLEV at a constant setpoint of 5 m^3. The PSE setpoint is reduced in order to increase the average throughput. The dashed lines indicate the constraints on the variable and the vertical dotted lines indicate the start of the disturbance events. The dash-dot line indicates the setpoint.

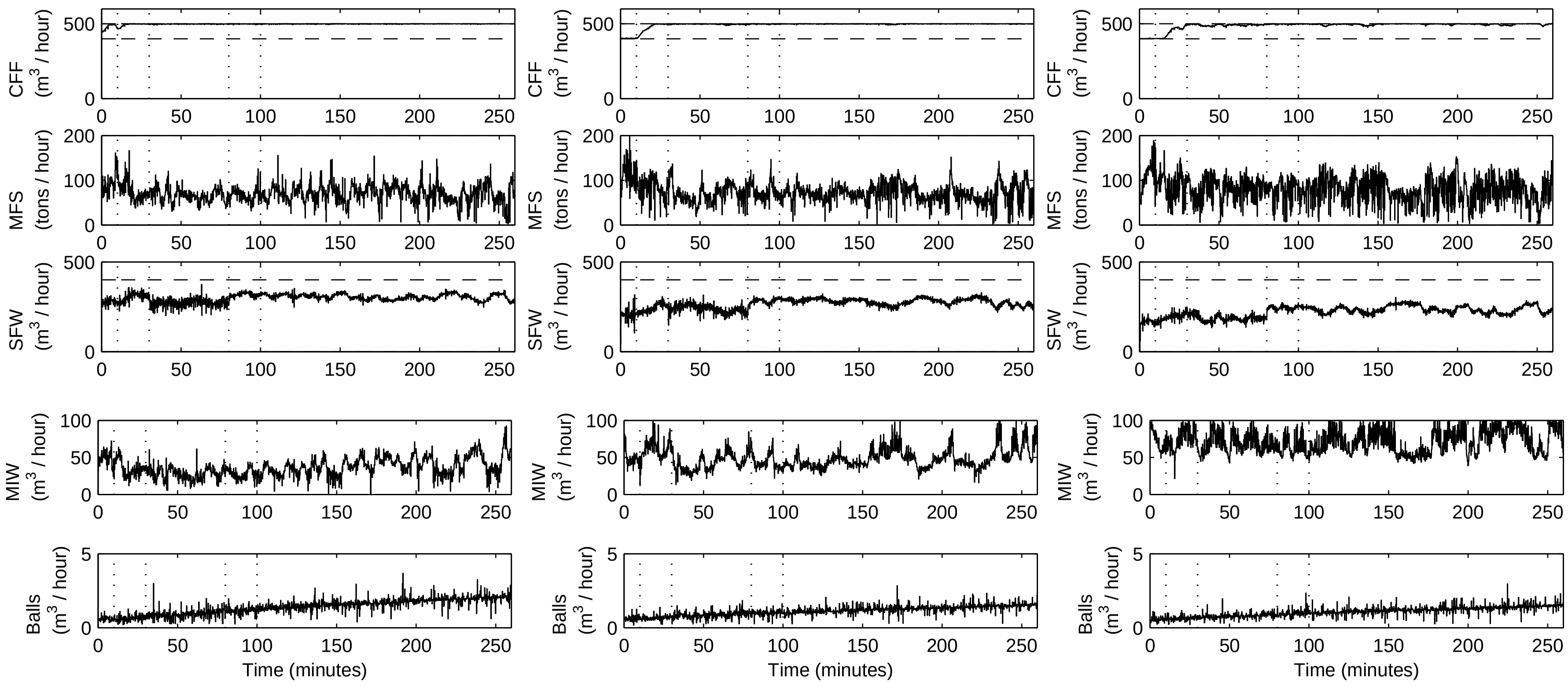

(a) PSE at 80. (b) PSE at 75. (c) PSE at 70.

Figure 5.17: MVs of the RNMPC.
The RNMPC regulates PSE at a constant setpoint of 80% (a), 75% (b) and 70% (c) with LOAD at a constant setpoint of 45% and SLEV at a constant setpoint of 5 m^3. The PSE setpoint is reduced in order to increase the average throughput. The dashed lines indicate the constraints on the variable and the vertical dotted lines indicate the start of the disturbance events. The dash-dot line indicates the setpoint.

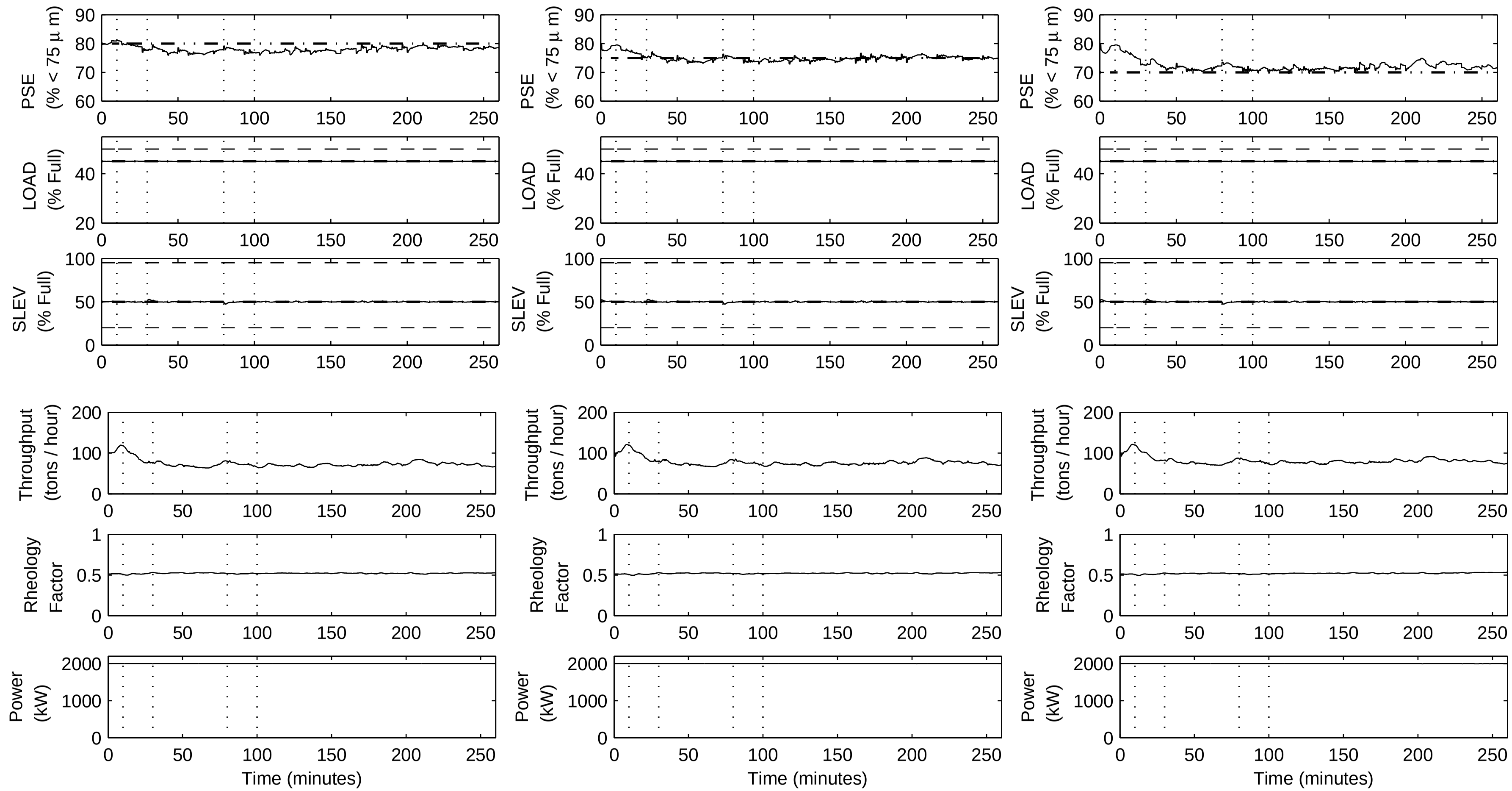

(a) PSE at 80.

(b) PSE at 75.

(c) PSE at 70.

Figure 5.18: CVs of PI controllers.

The PI controllers regulate PSE at a constant setpoint of 80% (a), 75% (b) and 70% (c) with LOAD at a constant setpoint of 45% and SLEV at a constant setpoint of 5 m^3. The PSE setpoint is reduced in order to increase the average throughput. The dashed lines indicate the constraints on the variable and the vertical dotted lines indicate the start of the disturbance events. The dash-dot line indicates the setpoint.

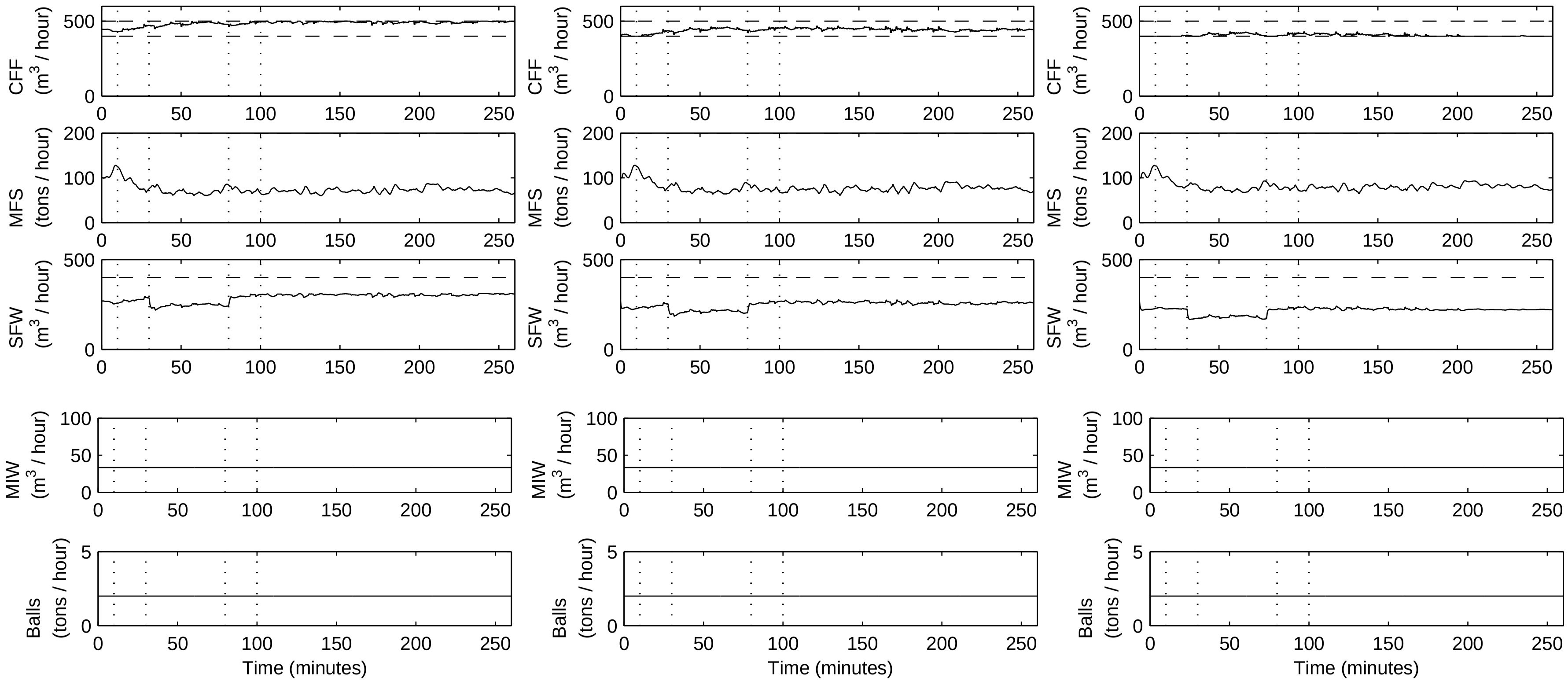

(a) PSE at 80. (b) PSE at 75. (c) PSE at 70.

Figure 5.19: MVs of PI controllers.
The PI controllers regulate PSE at a constant setpoint of 80% (a), 75% (b) and 70% (c) with LOAD at a constant setpoint of 45% and SLEV at a constant setpoint of 5 m^3. The PSE setpoint is reduced in order to increase the average throughput. The dashed lines indicate the constraints on the variable and the vertical dotted lines indicate the start of the disturbance events. The dash-dot line indicates the setpoint.

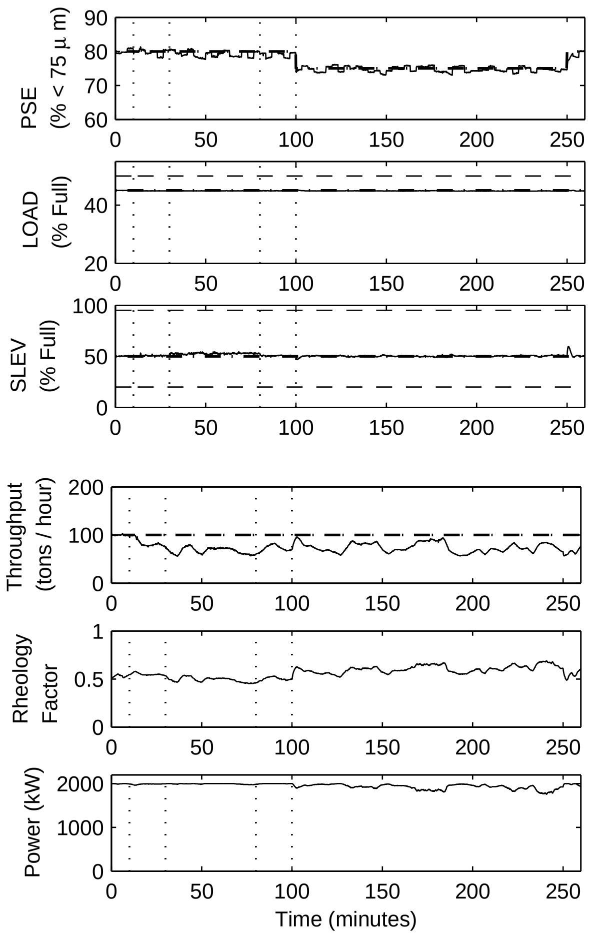

(a) RNMPC

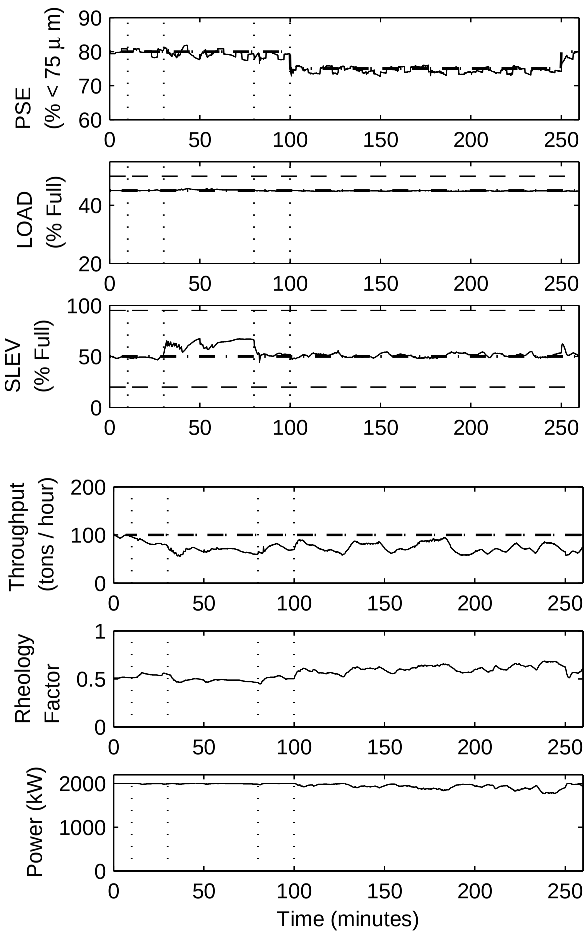

(b) NMPC

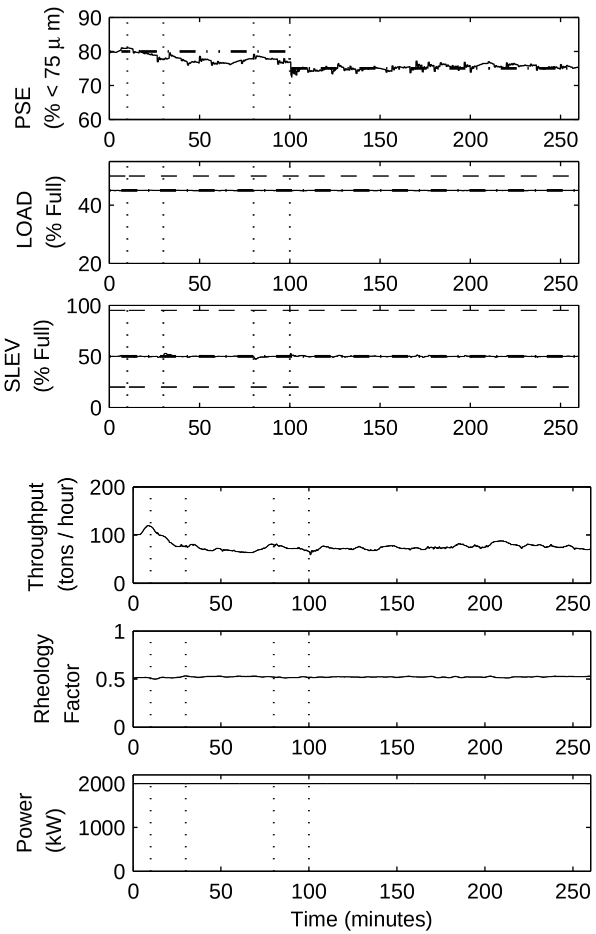

(c) PI controllers.

Figure 5.20: CVs of RNMPC (a), NMPC (b) and PI controllers (c).
The RNMPC and PI controllers follow a setpoint change from 80%-75% in PSE while maintaining LOAD and SLEV at a constant setpoint of 45% and 5 m^3 respectively. The dashed lines indicate the constraints on the variable and the vertical dotted lines indicate the start of the disturbance events. The dash-dot line indicates the setpoint.

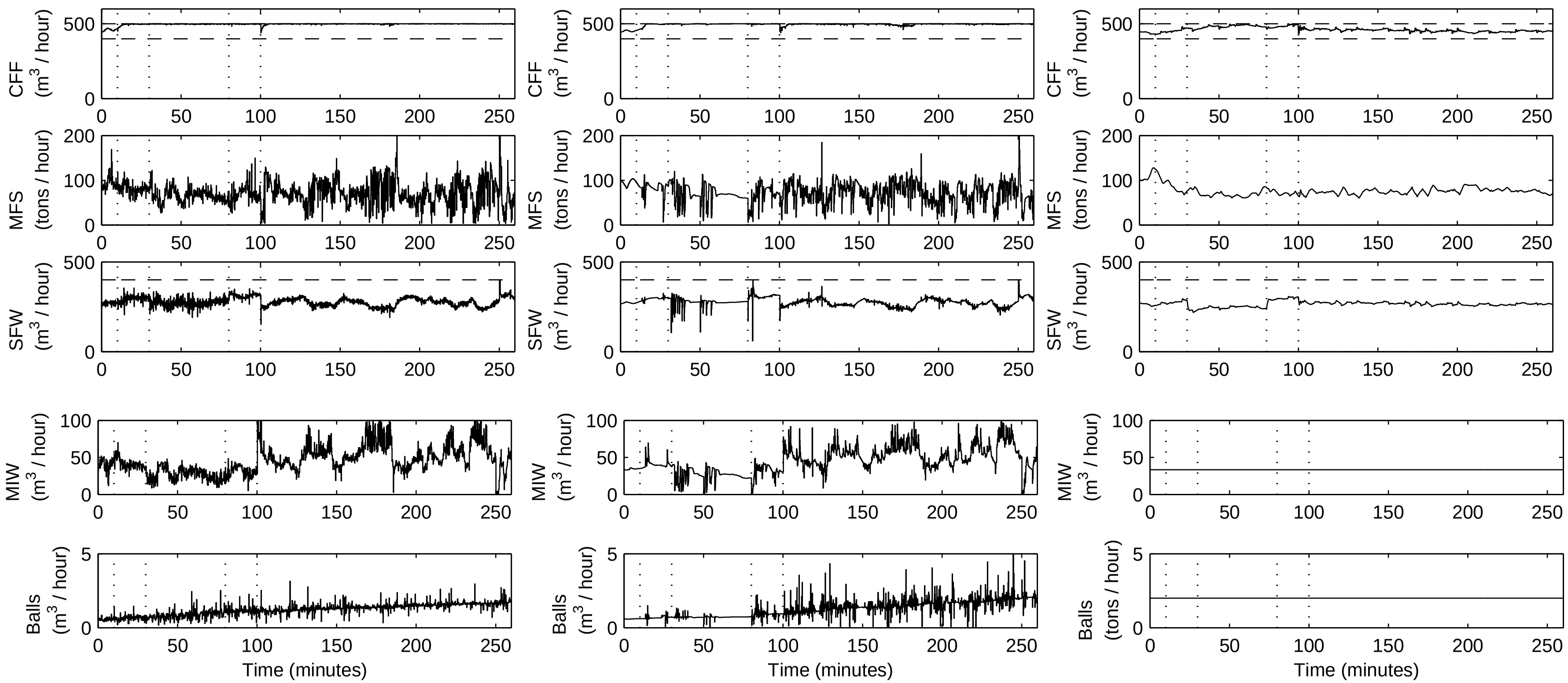

(a) RNMPC

(b) NMPC

(c) PI controllers.

Figure 5.21: MVs of RNMPC (a), NMPC (b) and PI controllers (c).
The RNMPC and PI controllers follow a setpoint change from 80%-75% in PSE while maintaining LOAD and SLEV at a constant setpoint of 45% and 5 m^3 respectively. The dashed lines indicate the constraints on the variable and the vertical dotted lines indicate the start of the disturbance events. The dash-dot line indicates the setpoint.

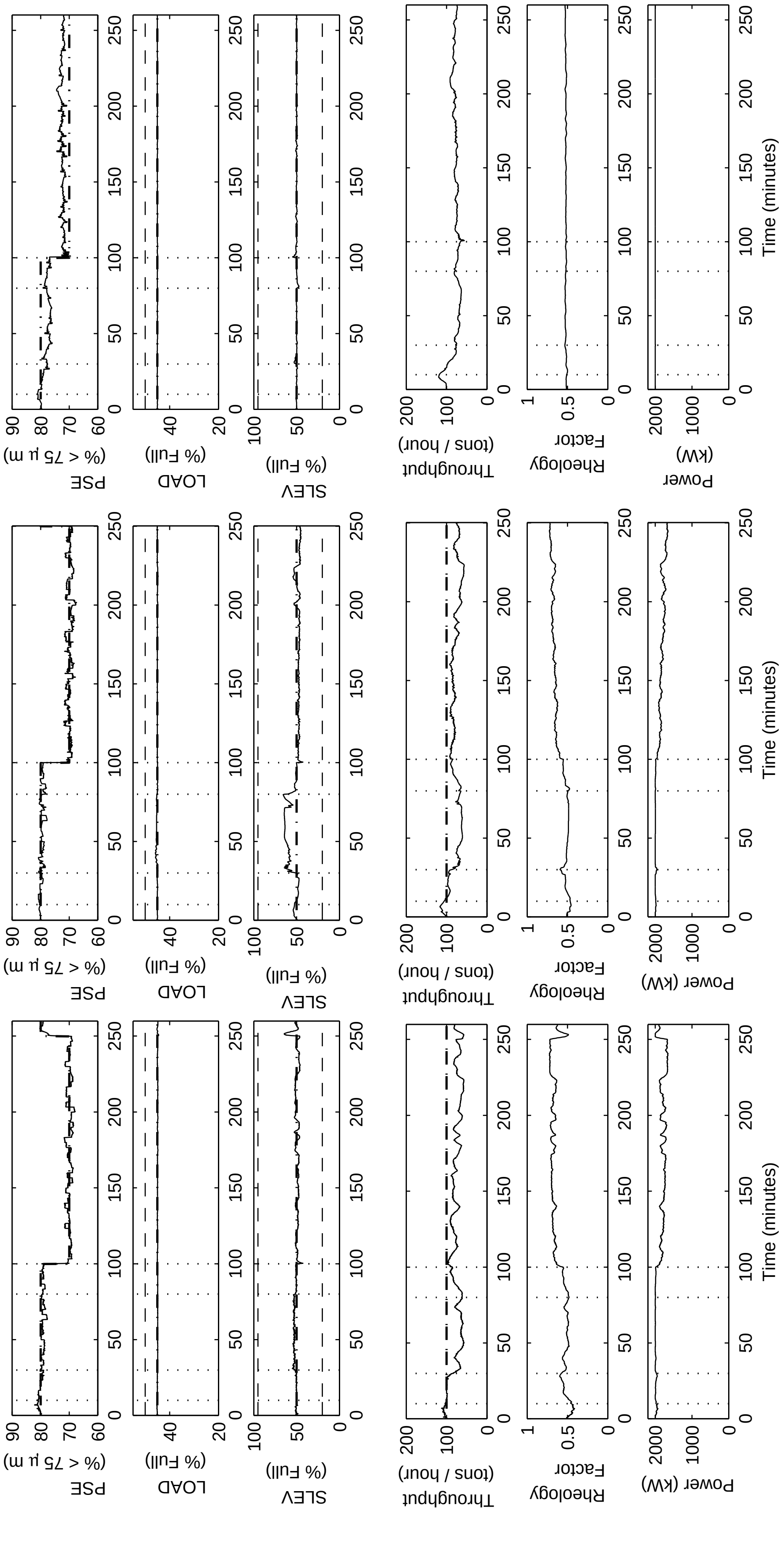

(a) RNMPC

(b) NMPC

(c) PI controllers.

Figure 5.22: CVs of RNMPC (a), NMPC (b) and PI controllers (c). The RNMPC and PI controllers follow a setpoint change from 80%-70% in PSE while maintaining LOAD and SLEV at a constant setpoint of 45% and 5 m^3 respectively. The dashed lines indicate the constraints on the variable and the vertical dotted lines indicate the start of the disturbance events. The dash-dot line indicates the setpoint.

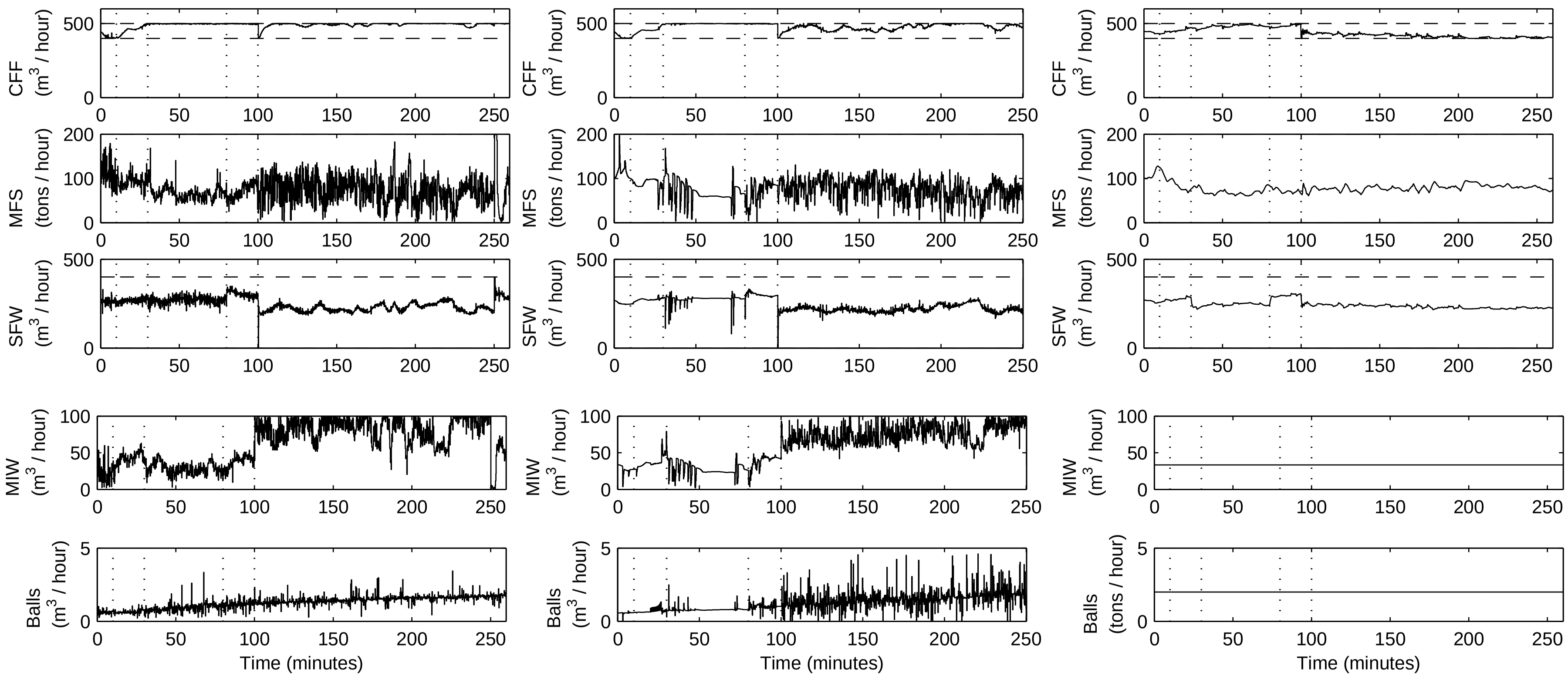

(a) RNMPC (b) NMPC (c) PI controllers.

Figure 5.23: MVs of RNMPC (a), NMPC (b) and PI controllers (c).
The RNMPC and PI controllers follow a setpoint change from 80%-70% in PSE while maintaining LOAD and SLEV at a constant setpoint of 45% and 5 m^3 respectively. The dashed lines indicate the constraints on the variable and the vertical dotted lines indicate the start of the disturbance events. The dash-dot line indicates the setpoint.

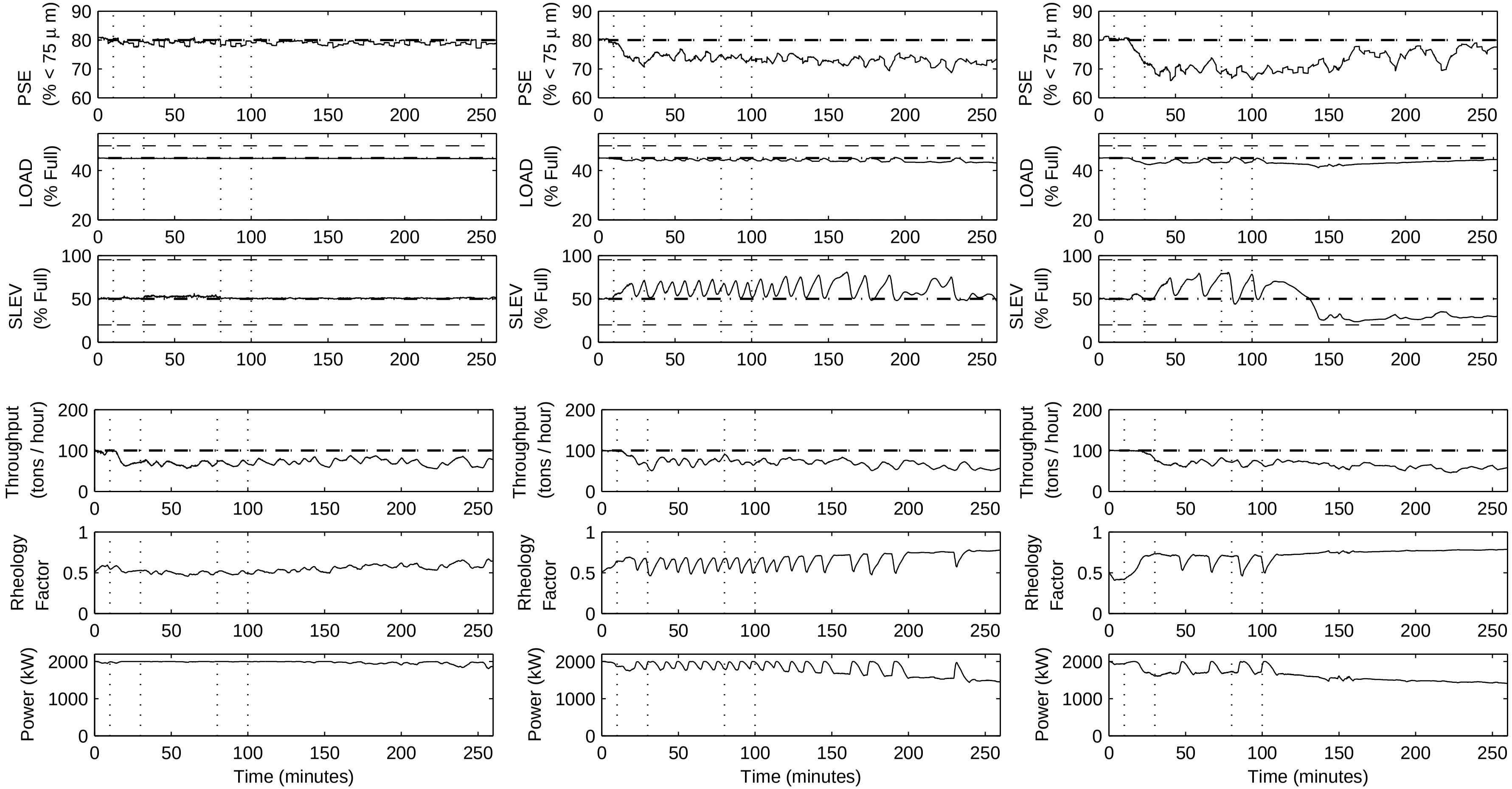

(a) THROUGHPUT weighting 5.

(b) THROUGHPUT weighting 10.

(c) THROUGHPUT weighting 20.

Figure 5.24: CVs of the RNMPC.
The RNMPC regulates PSE and LOAD at constant setpoints and throughout at a constant setpoint of 100 tons/hour. The weighting of THROUGHPUT in the objective function is 5 (a), 10 (b) and 20 (c), while the weighting on PSE and LOAD is 100 respectively. The optimising property of the RNMPC is employed to try and increase throughput without affecting PSE. An increase in THROUGHPUT, however, caused a decrease in PSE. The dashed lines indicate the constraints on the variable and the vertical dotted lines indicate the start of the disturbance events. The dash-dot line indicates the setpoint.

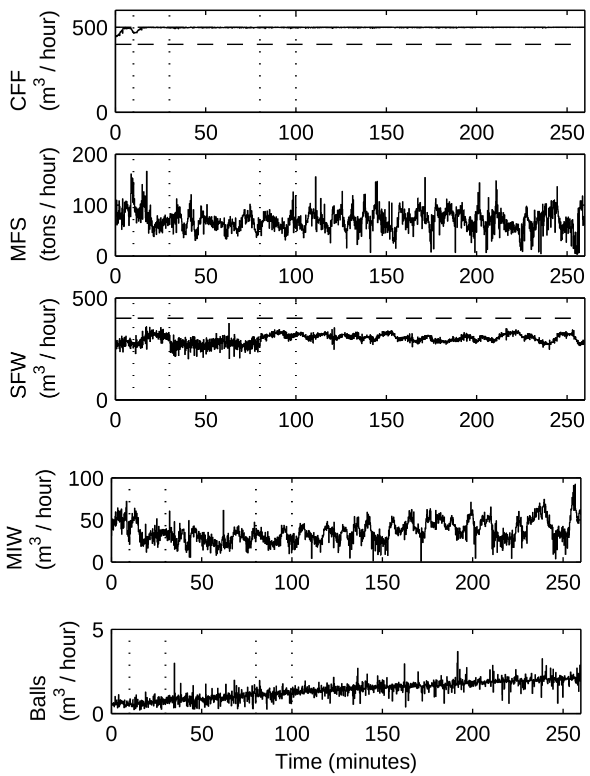

(a) THROUGHPUT weighting 5.

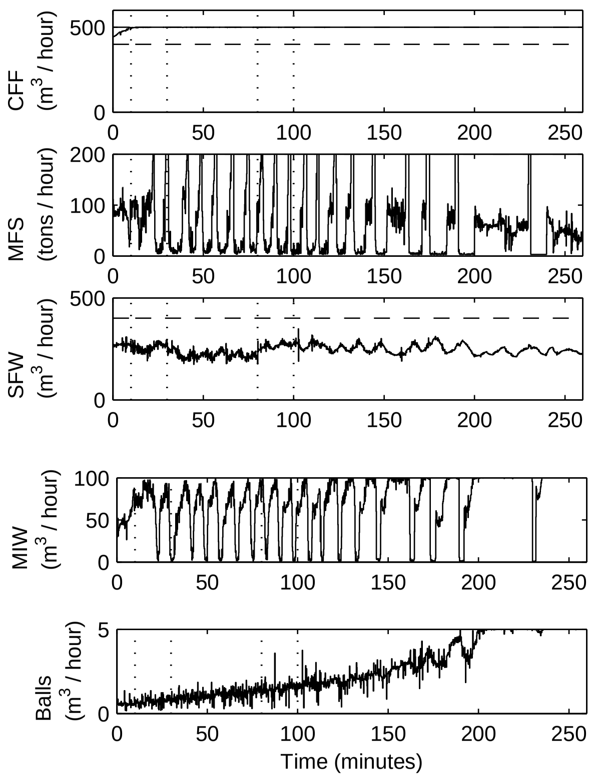

(b) THROUGHPUT weighting 10.

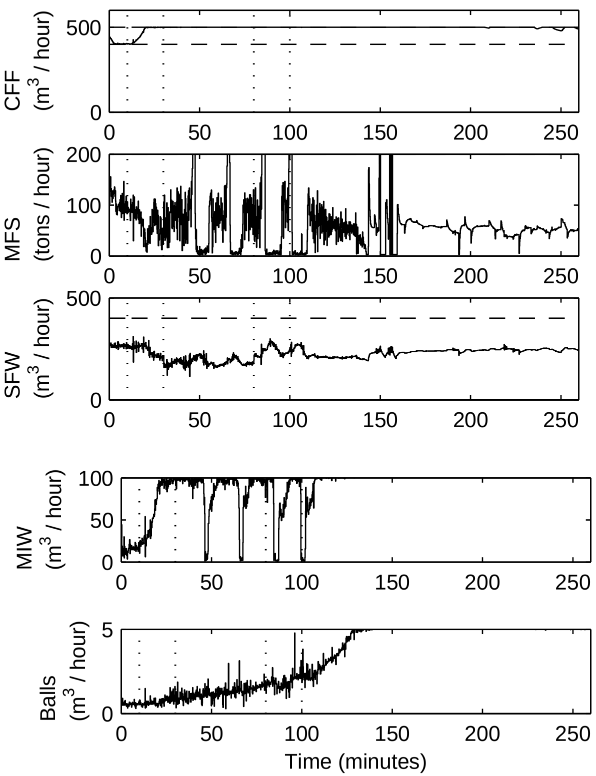

(c) THROUGHPUT weighting 20.

Figure 5.25: MVs of the RNMPC.
The RNMPC regulates PSE and LOAD at constant setpoints and throughout at a constant setpoint of 100 tons/hour. The weighting of THROUGHPUT in the objective function is 5 (a), 10 (b) and 20 (c), while the weighting on PSE and LOAD is 100 respectively. Increasing the weighting on THROUGHPUT caused increasingly oscillatory behaviour in the MVs. The dashed lines indicate the constraints on the variable and the vertical dotted lines indicate the start of the disturbance events. The dash-dot line indicates the setpoint.

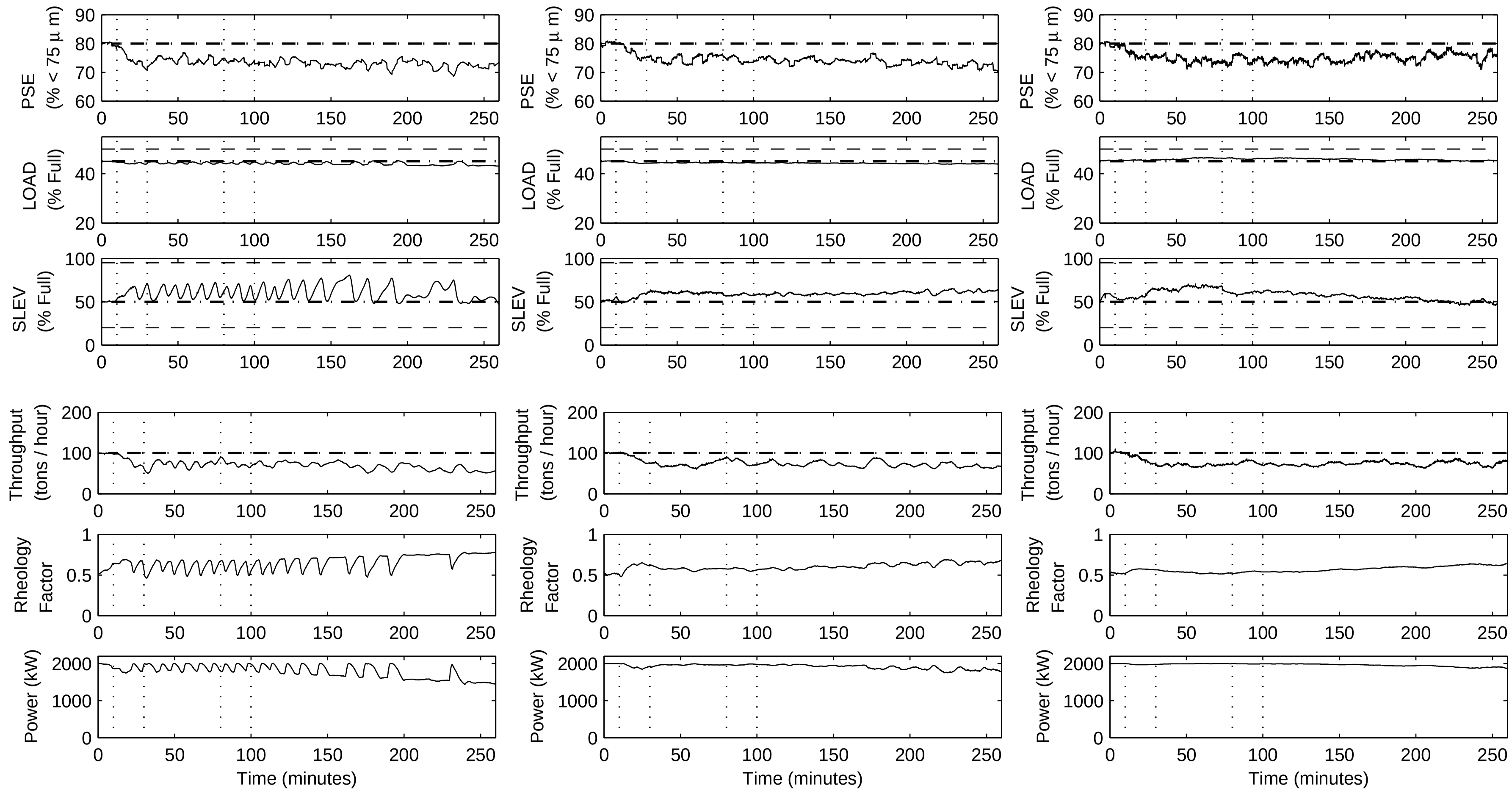

(a) MV weighting weighting 0.01.

(b) MV weighting weighting 0.1.

(c) MV weighting weighting 1.0.

Figure 5.26: CVs of the RNMPC.
The weighting on the MVs are increased from 0.01 (a) to 0.1 (b) and 1.0 (c) in order to reduce the oscillation in the MVs. The increased weighting on the MVs results in better tracking of PSE and higher average THROUGHPUT. The dashed lines indicate the constraints on the variable and the vertical dotted lines indicate the start of the disturbance events. The dash-dot line indicates the setpoint.

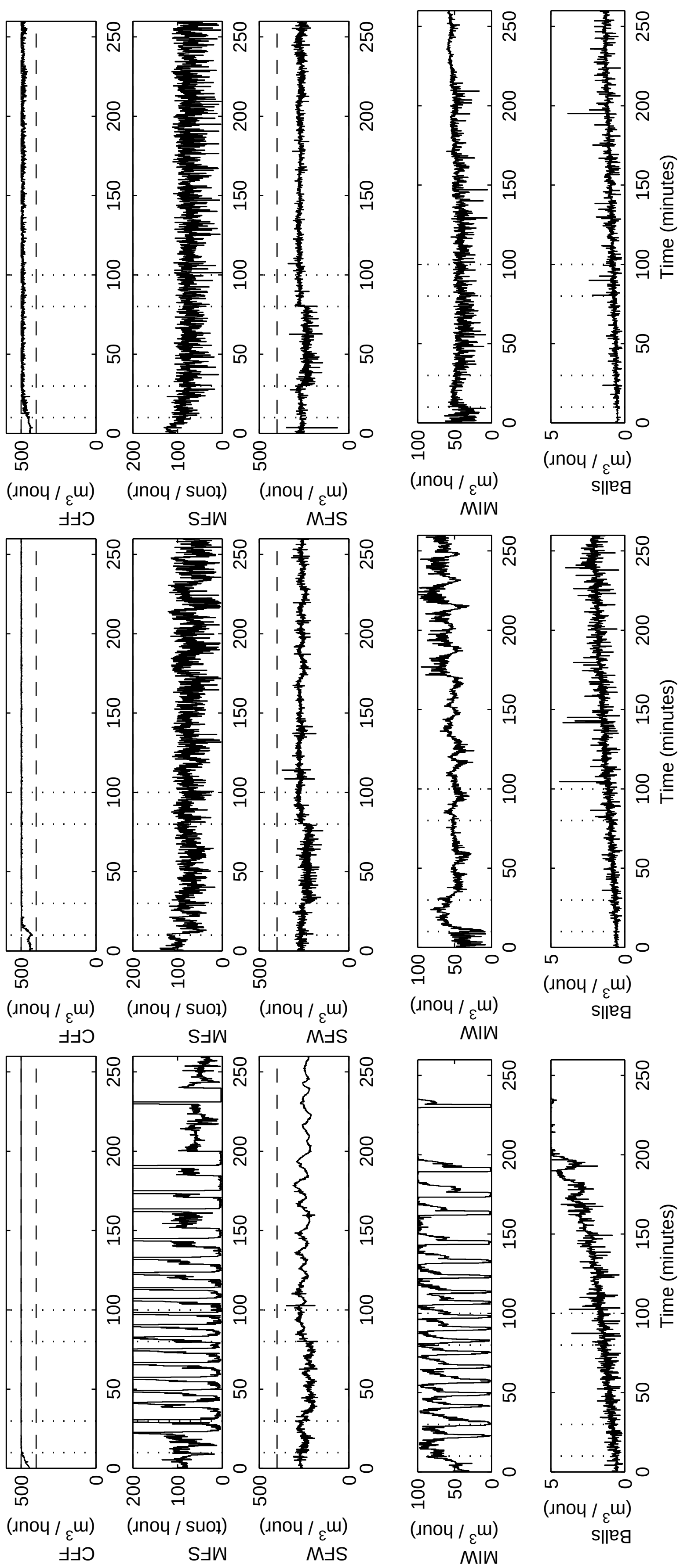

(a) MV weighting weighting 0.01.

(b) MV weighting weighting 0.1.

(c) MV weighting weighting 1.0.

Figure 5.27: MVs of the RNMPC.

The weighting on the MVs is increased from 0.01 (b) to 0.1 (b) and 1.0 (c) in order to reduce the oscillation in the MVs. The increased weighting on the MVs results in better tracking of PSE and higher average THROUGHPUT. The dashed lines indicate the constraints on the variable and the vertical dotted lines indicate the start of the disturbance events. The dash-dot line indicates the setpoint.

5.4 DISCUSSION

The simulation results in this chapter may lead to some questions regarding the choices of the disturbances and controller design. This section aims to answer some of the questions that come to mind.

The step disturbance in ore hardness leads to CFF saturation in most of the simulations. Feed ore hardness and composition changes are major disturbances that milling circuit controllers have to contend with, as could happen when the feed ore is switched between feeds that originate from different stockpiles containing different ore types. The step disturbances are therefore chosen to simulate these disturbances.

The single-loop PI controller responsible for controlling the PSE-CFF loop exhibits a slow response. The PSE-CFF loop is characterised by a non-minimum phase response, as seen in Section 4.3.1. Tuning the PI controller more aggressively than recommended by the SIMC tuning method resulted in poorer performance. The limiting factor for tuning the PI controller is therefore the non-minimum phase response exhibited by the model.

It does not seem necessary to control SLEV, because the use of such a reservoir is to absorb disturbances, which is not done when its level is controlled. RNMPC and NMPC can be configured to allow SLEV to vary freely between upper and lower bounds. The scenario where SLEV is allowed to vary freely was investigated in Section 5.3.2 and found not to improve performance significantly. The weighting of SLEV compared to PSE and LOAD is significantly less, which allows the controller to vary SLEV in order to maintain PSE and LOAD at setpoint, as seen in Figure 5.26.

The performance of the PI controllers can be improved by using simple MIMO compensators. A recent survey by Wei and Craig (2009), however, reported that more than 60% of all respondents still only use PI control for grinding mill circuit control, usually single-loop PI controllers. This study aimed to determine the advantage that multivariable control, in the form of RNMPC and NMPC, may provide over SISO control, such as single-loop PI control, which is still employed in the majority of grinding circuits.

Figure 5.1 shows an example of typical parameter variations graphically, as employed in the simulations. The parameter variations were chosen to be uniformly distributed, because this results in a large change from one parameter vector to the next. The parameters are kept constant for a long enough period to allow the new parameter values to propagate through the process and affect its response.

MIW shows large variations that are not typically allowed in practice (Craig *et al.*, 1992*a*). The MIW is usually ratio-controlled to the MFS to maintain a relatively constant solids-to-water ratio inside the mill. Craig *et al.* (1992*a*) showed that MIW can be used to extend the control of PSE. For the simulation studies presented in this thesis, full authority of MIW was, therefore, given to the MPC controllers in order to determine if MIW can be used to increase control of the important variables, such as PSE and THROUGHPUT.

The manipulated variables of the RNMPC and NMPC show spikes. Figure 5.28 and Figure 5.29 enlarge a relatively spiky region of Figure 5.2 and Figure 5.3 between time 95 minutes and 105 minutes, showing that the spikes are not as severe as it seem from the full-length simulation results. The RNMPC show much less variation in the MVs than the NMPC, because RNMPC employ rate constraints as shown in the Δ column of Table 5.1. The rate constraints do not seem to have an impact on the performance of the RNMPC negatively compared to the NMPC. The spikes can be reduced further by filtering the measured variables used by the controllers. Mhaskar and Kennedy (2008) warn, however, that rate constraints can affect the closed-loop stability of the system if they are not incorporated correctly into the controller formulation.

The performance of the NMPC controller is very similar to the performance of the RNMPC controller. Some of the differences can be attributed to the ability of the RNMPC to handle rate constraints on the MVs. The RNMPC did not exhibit any significant stability or performance advantage in a majority of the simulations over the NMPC, which leads to the conclusion that the NMPC controller is more than adequate for controlling the ROM milling circuit presented here.

Nonlinear control can be justified by noting that the cyclone model (Section 2.3.4.4) and the mill power draw function (equation (2.27)) are static nonlinear models that will reduce to constant gains when linearised and will, therefore, only be accurate in a small region around the operating point. Static nonlinear models in the form of efficiency curves are used to model a number of classification units in minerals processing, such as cyclones (Nageswararao *et al.*, 2004) and screens. Nonlinear controllers, such as NMPC and RNMPC, have the advantage of being able to use these static nonlinear models directly as internal prediction models ensuring accurate results over a larger operating window.

5.5 SIMULATION SUMMARY

A summary of the simulation results are given in Table 5.4 that details the tracking performance of the controller with regard to the PSE, LOAD and throughput. The simulation scenarios are outlined in terms of the controlled variable weighting and setpoint values, as well as the step disturbances. The relevant changes in each simulation scenario are highlighted in bold. The dashes in the table represent values that are either zero or not applicable. The performance metrics are described in Section 5.2.

The headings of Table 5.4 are defined as

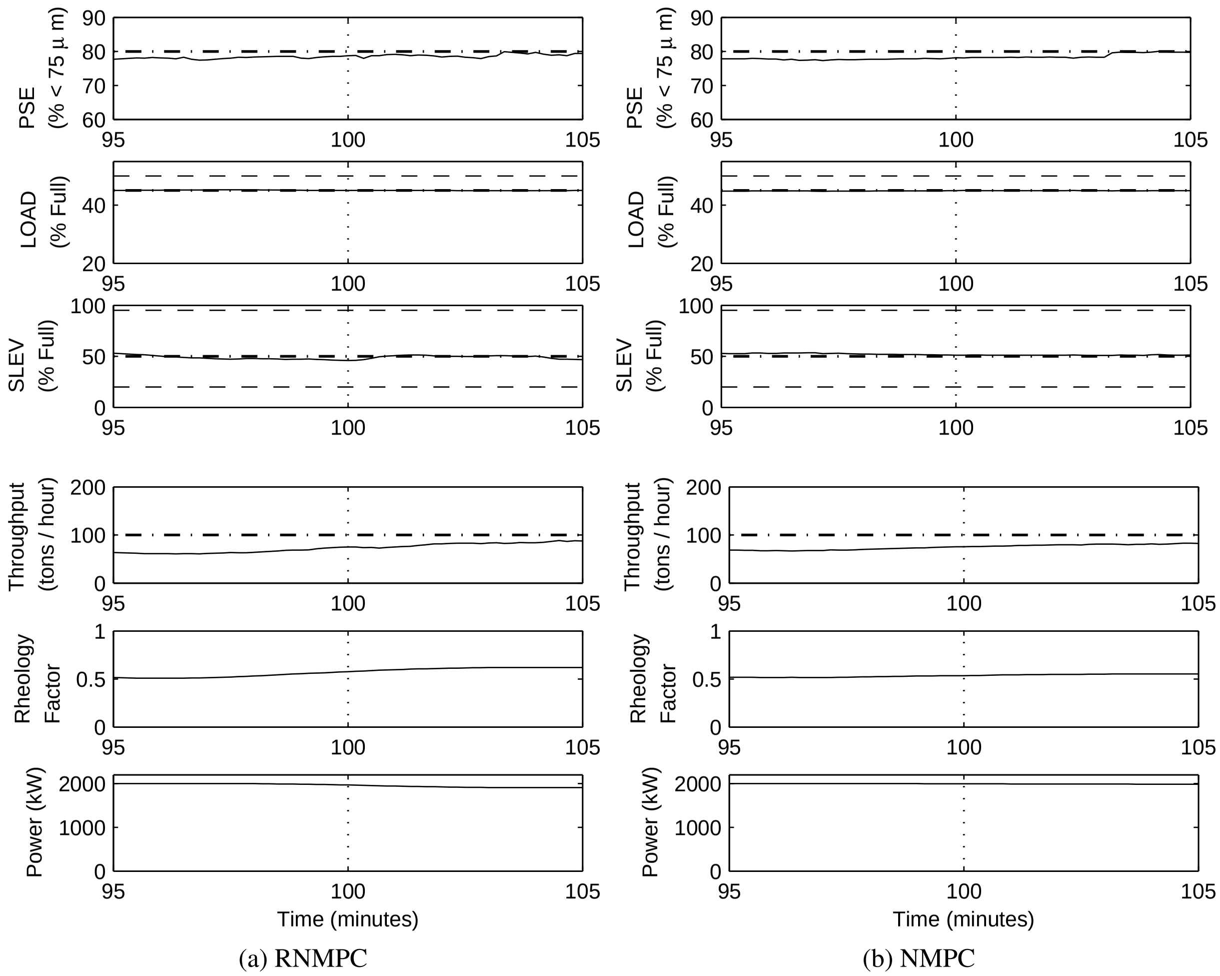

Figure 5.28: CVs of RNMPC (a) and NMPC (b) controllers.
Feed ore hardness and composition step disturbances are present as well as a sump feed water disturbance simulating spillage water being added to the sump. This simulation show the results from 95 minutes to 105 minutes of Figure 5.2. The dashed lines indicate the constraints on the variable and the vertical dotted lines indicate the start of the disturbance events. The dash-dot line indicates the setpoint.

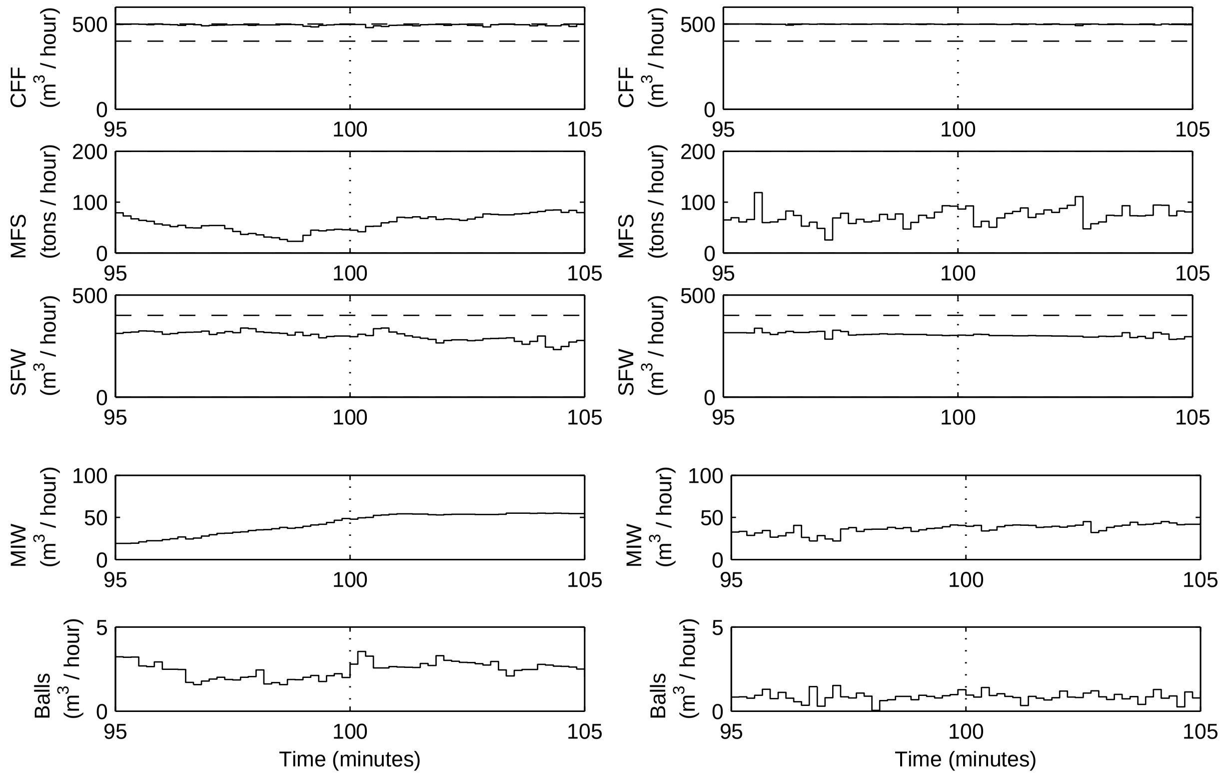

(a) RNMPC (b) NMPC

Figure 5.29: MVs of RNMPC (a) and NMPC (b) controllers.
Feed ore hardness and composition step disturbances are present as well as a sump feed water disturbance simulating spillage water being added to the sump. This simulation show the results from 95 minutes to 105 minutes of Figure 5.3. The dashed lines indicate the constraints on the variable and the vertical dotted lines indicate the start of the disturbance events. The dash-dot line indicates the setpoint.

PSE	Particle Size Estimate. [$\% < 75\mu$m]
LOAD	The volumetric filling of the mill. [%]
Throughput	The amount of solids discharged at the cyclone overflow. [tons/hour]
SLEV	Sump level. [m^3]
Power	The electrical power draw of the mill motor. [kW]
Rheology	An indication of the fluidity of the slurry inside the mill. [fraction]
U	The manipulated variables.
Disturbances	Describes the step disturbances in ore hardness, fraction of rocks in the feed ore and SFW.
Time	Describes the average and maximum iteration time of the simulations [seconds].

The subheadings of Table 5.4 are defined as

Δ	The sum of the squares of the error from the setpoint.
S	The setpoint of the variable.
W	The weight of the variable in the objective function.
A	The average value of the variable over the simulation duration.
RH	The increase in the hardness of the feed ore. [%]
AR	The increase in the fraction of rocks in the feed ore. [%]
SFW	The increase in SFW. [m^3/hour]
T	The time when the disturbance is introduced.
M	The maximum value of the variable over the simulation duration.

The controllers are identified next to the figure numbers in Table 5.4 by

R	Robust Nonlinear Model Predictive Controller.
N	Nonlinear Model Predictive Controller.
P	Proportional-Integral-Differential Controller.

The simulations show that RNMPC and NMPC are capable of tighter control of PSE, especially when constraints are active, because the multivariable controllers can leverage the multivariable nature of the milling circuit to increase the control envelope. The RNMPC and NMPC controllers are, however, not capable of improving throughput while maintaining PSE at the desired setpoint. The PI controllers showed very good performance for SISO control, because they were tuned very aggressively. In certain milling circuits there are large time delays that will only allow less aggressive tuning of the PI controllers, resulting in degraded performance. MPC controllers were found in practice to provide good performance over longer periods compared to PI controllers (Chen *et al.*, 2007*b*, Ramasamy *et al.*, 2005).

Some additional simulation scenarios are considered in Section B.2.

Table 5.4: Simulation summary.

			PSE			LOAD			Throughput			SLEV		Power		Rheology		U	Disturbances						Time	
Simulation			Δ	S	W	Δ	S	W	A	S	W	S	W	S	W	S	W	W	RH	T	AR	T	S	T	A	M
Figure 5.4	a	**R**	0.05	80	100	2.90E-05	45	100	106.72	99.9	0	5	**0**	2000	0	0.51	0	0.01	—	—	—	—	—	—	12.8	132
Figure 5.5	b	**R**	0.05	80	100	3.50E-05	45	100	111.00	99.9	0	5	**1**	2000	0	0.51	0	0.01	—	—	—	—	—	—	22.6	186
	c	**P**	0.15	80	—	5.35E-04	45	—	106.28	—	—	5	**—**	—	—	—	—	—	—	—	—	—	—	—	—	—
Figure 5.6	a	**R**	0.07	80	100	3.30E-05	45	100	88.71	99.9	0	5	1	2000	0	0.51	0	0.01	**50**	**180**	—	—	—	—	21.7	318
Figure 5.7	b	**N**	0.08	80	100	2.40E-05	45	100	88.97	99.9	0	5	1	2000	0	0.51	0	0.01	**50**	**180**	—	—	—	—	0.1	1.52
	c	**P**	0.97	80	—	4.58E-04	45	—	95.67	—	—	5	—	—	—	—	—	—	**50**	**180**	—	—	—	—	—	—
Figure 5.8	a	**R**	0.05	80	100	4.00E-05	45	100	103.5	99.9	0	5	1	2000	0	0.51	0	0.01	—	—	**50**	**180**	—	—	24.5	204
Figure 5.9	b	**N**	0.09	80	100	7.30E-05	45	100	102.86	99.9	0	5	1	2000	0	0.51	0	0.01	—	—	**50**	**180**	—	—	0.1	1.56
	c	**P**	0.18	80	—	5.82E-04	45	—	105.53	—	—	5	—	—	—	—	—	—	—	—	**50**	**180**	—	—	—	—
Figure 5.10	a	**R**	0.06	80	100	4.40E-05	45	100	103.26	99.9	0	5	1	2000	0	0.51	0	0.01	—	—	**50**	**10**	—	—	27.1	291
Figure 5.11	b	**N**	0.23	80	100	3.06E-04	45	100	101.77	99.9	0	5	1	2000	0	0.51	0	0.01	—	—	**50**	**10**	—	—	0.1	1.47
	c	**P**	0.41	80	—	6.32E-04	45	—	106.96	—	—	5	—	—	—	—	—	—	—	—	**50**	**10**	—	—	—	—
Figure 5.12	a	**R**	0.05	80	100	4.40E-05	45	100	110.89	99.9	0	5	1	2000	0	0.51	0	0.01	—	—	**0**	—	**50**	**180**	26.7	340
Figure 5.13	b	**N**	0.08	80	100	6.60E-05	45	100	110.28	99.9	0	5	1	2000	0	0.51	0	0.01	—	—	**0**	—	**50**	**180**	0.1	1.59
	c	**P**	0.16	80	—	7.71E-04	45	—	110.30	—	—	5	—	—	—	—	—	—	—	—	**0**	—	**50**	**180**	—	—
Figure 5.14	a	**R**	0.23	80	100	2.03E-03	45	100	72.22	99.9	1	5	1	2000	0	0.51	0	0.01	**50**	**10**	**50**	**100**	**50**	**30-80**	34.9	1014
Figure 5.15	b	**N**	0.3	80	100	1.76E-03	45	100	72.58	99.9	1	5	1	2000	0	0.51	0	0.01	**50**	**10**	**50**	**100**	**50**	**30-80**	0.2	1.77
	c	**P**	0.77	80	—	1.52E-04	45	—	74.59	—	—	5	—	—	—	—	—	—	**50**	**10**	**50**	**100**	**50**	**30-80**	—	—
Figure 5.16	a	R	0.23	**80**	100	2.03E-03	45	100	72.22	99.9	1	5	1	2000	0	0.51	0	0.01	50	10	50	100	50	30-80	34.9	1014
Figure 5.17	b	R	0.12	**75**	100	1.54E-03	45	100	74.51	99.9	1	5	1	2000	0	0.51	0	0.01	50	10	50	100	50	30-80	35.9	1132
	c	R	0.12	**70**	100	9.33E-04	45	100	81.35	99.9	1	5	1	2000	0	0.51	0	0.01	50	10	50	100	50	30-80	33.4	1136
Figure 5.18	a	P	0.77	**80**	—	1.52E-04	45	—	74.59	—	—	5	—	—	—	—	—	—	50	10	50	100	50	30-80	—	—
Figure 5.19	b	P	0.24	**75**	—	1.62E-04	45	—	77.98	—	—	5	—	—	—	—	—	—	50	10	50	100	50	30-80	—	—
	c	P	1.50	**70**	—	1.40E-04	45	—	81.20	—	—	5	—	—	—	—	—	—	50	10	50	100	50	30-80	—	—
Figure 5.20	a	**R**	0.15	**80→75**	100	1.65E-03	45	100	74.04	99.9	1	5	1	2000	0	0.51	0	0.01	50	10	50	100	50	30-80	33.8	688
Figure 5.21	b	**N**	0.18	**80→75**	100	1.55E-03	45	100	74.22	99.9	1	5	1	2000	0	0.51	0	0.01	50	10	50	100	50	30-80	9.6	58
	c	**P**	0.39	**80→75**	—	1.64E-04	45	—	76.43	—	—	5	—	—	—	—	—	—	50	10	50	100	50	30-80	—	—
Figure 5.22	a	**R**	0.15	**80→70**	100	1.42E-03	45	100	76.73	99.9	1	5	1	2000	0	0.51	0	0.01	50	10	50	100	50	30-80	39.3	1127
Figure 5.23	b	**N**	0.14	**80→70**	100	1.21E-03	45	100	78.11	99.9	1	5	1	2000	0	0.51	0	0.01	50	10	50	100	50	30-80	10.3	70
	c	**P**	0.92	**80→70**	—	1.74E-04	45	—	78.52	—	—	5	—	—	—	—	—	—	50	10	50	100	50	30-80	—	—
Figure 5.24	a	R	2.79	80	100	1.55E-02	45	100	71.14	99.9	**5**	5	1	2000	0	0.51	0	0.01	50	10	50	100	50	30-80	21.0	813
Figure 5.25	b	R	7.09	80	100	3.44E-02	45	100	70.76	99.9	**10**	5	1	2000	0	0.51	0	0.01	50	10	50	100	50	30-80	15.2	619
	c	R	10.01	80	100	6.85E-02	45	100	68.09	99.9	**20**	5	1	2000	0	0.51	0	0.01	50	10	50	100	50	30-80	13.3	682
Figure 5.26	a	R	7.09	80	100	3.44E-02	45	100	70.76	99.9	**10**	5	1	2000	0	0.51	0	**0.01**	50	10	50	100	50	30-80	15.2	619
Figure 5.27	b	R	5.52	80	100	2.62E-02	45	100	74.85	99.9	**10**	5	1	2000	0	0.51	0	**0.1**	50	10	50	100	50	30-80	49.2	1215
	c	R	4.11	80	100	2.47E-02	45	100	75.6	99.9	**10**	5	1	2000	0	0.51	0	**1.0**	50	10	50	100	50	30-80	33.2	987

CHAPTER 6

CONCLUSIONS AND FURTHER WORK

6.1 SUMMARY AND EVALUATION

Advanced control such as MPC has not been as readily adopted by the mineral-processing industry as compared to, for example, the petrochemical industry (Wei and Craig, 2009). This thesis investigated the feasibility of applying RNMPC to a ROM ore milling circuit and the conditions under which such a controller might be worthwhile implementing.

A comprehensive modularised ROM ore milling circuit model was described in Section 2.3.4 and cast into an RNMPC framework. The results of practically motivated simulations presented in Chapter 5 show that an RNMPC controller can successfully control important milling circuit variables in the face of large disturbances that are not uncommon in practice.

The adoption of advanced control by the mineral processing industry will probably be determined by the trade-off between the added complexity of implementing and maintaining an advanced controller such as RNMPC and the benefits that can be derived from such an implementation. Results given in this thesis suggest that if a milling circuit regularly experiences large feed ore hardness and composition changes, when for example the feed ore is switched between feeds that originate from different stockpiles, RNMPC might well warrant a closer look.

6.1.1 Strong points

The RNMPC was successfully implemented by using an open-source package called IPOPT (Kawajir *et al.*, 2006) for large-scale nonlinear parameter optimisation and an open-source package called CPPAD (Lougee-Heimer, 2003) for calculating the derivatives of $g(\cdot)$ as well as solving the differential equation (6.1) by integration. The efficiency of the algorithm is obtained by structuring the problem correctly (Section 3.7.3) and minimising unnecessary calculations by keeping track of the available results and only returning the results if these are already available, rather than recalculating them.

RNMPC can explicitly take model uncertainty into account as part of the prediction model. This allows RNMPC to be more robust against model uncertainty and process disturbances.

The results shown in Chapter 5 and Addendum B and summarised in Addendum D suggest that if a milling circuit regularly experiences large feed ore hardness and composition changes, when for example the feed ore is switched between feeds that originate from different stockpiles, RNMPC may provide better performance than PI controllers. RNMPC can extend the operation envelope of the process when constraints become active to maintain the performance of the process.

RNMPC can under certain conditions provide better performance compared to NMPC, as seen in the simulation results (Addendum D), because it optimises over the worst-case realisation of the system.

RNMPC can avoid conditions in the milling circuit that affect production negatively, such as mill overload conditions, because it can enforce state and output constraints. RNMPC can therefore use the sump to stabilise the slurry density before pumping it to the cyclone, effectively increasing the operational envelope of the milling circuit. This is accomplished by varying the sump level within its limits. PI control cannot achieve any of these two feats, because it cannot enforce constraints on the outputs.

RNMPC can incorporate almost any nonlinear model without major modifications (such as linearisation and conversion to a fixed structure). It even handles a nonlinear static model very well, such as the cyclone model, where most of the "dynamics" are lost when the model is linearised. Nonlinear static models are common in minerals processing, where cyclones and screens are usually modelled by efficiency equations (Wills and Napier-Munn, 2006). The RNMPC only requires the nonlinear model interface to be defined as

$$\dot{x}(t) = g(x(t), u(t), p(t)) \tag{6.1}$$

where $x(t)$ is the current state vector at time t, $\dot{x}(t)$ is the change in states at time t, $u(t)$ is the control vector at time t, and $p(t)$ the parameters at time t. The dimensions of the vectors $(x(t), u(t), p(t))$ may be of arbitrary size. The requirements on the nonlinear model are that the model should be stabilisable and twice continuous differentiable, but they do not impose any fixed structure on the model, which allows any arbitrary milling circuit to be simulated and controlled using this interface.

The RNMPC implementation presented in this thesis is parallel processor capable, which allows it to be sped up on multi-core/multi-processor systems. Complex systems can therefore be controlled with a sufficient investment in computer hardware.

Recent studies of applying MPC to ore milling circuits have shown that model predictive controllers provide better long-term stability than PI control (Chen *et al.*, 2007*a*, *b*, 2008).

Most industrial MPC controllers require brute-force simulation to evaluate the effects of model mismatch on closed-loop stability (Qin and Badgwell, 2003). Time spent tuning and testing of industrial controllers can, however, be significantly reduced if the controllers implement nominal and potentially robust stability measures, such as RNMPC, even though closed-loop stability of industrial MPC itself is not perceived to be a serious problem by industry practitioners (Qin and Badgwell, 2003).

6.1.2 Drawbacks

The simulation was executed at an average time of about 26 seconds and a maximum time of 123 seconds per iteration on a Dell PowerEdge 1955 blade with Intel Xeon 5140 (Dual-Core) 2.33GHz processor, 2GB RAM and 1333MHz FSB. This platform is typically faster than the implementation platforms available on most mineral-processing plants.

The current RNMPC implementation is not feasible for practical implementation, because the maximum and average calculation times are much longer than the recommended sampling time of 10 seconds (Craig and MacLeod, 1995). There are various factors that influence the calculation time. Increasing the prediction horizon T increases the calculation time because of an increase in total integration time. Increasing the number of nodes N significantly increases the computational time, because of an increase in the number of decision variables. The control horizon is determined by the number of nodes N, because the MVs are changed at each node. Tuning the controller will therefore need to include the selection of the prediction horizon T and number of nodes N for stability and performance, while maintaining a reasonable calculation time. With the continuous increase in computing power, this should become less of an issue in the foreseeable future.

The simulation further assumed full-state feedback, which is not available on real plants. Typically the controlled variables PSE, SLEV, LOAD and the cyclone feed or sump density would be measured online (Wei and Craig, 2009), from which an observer would need to infer the model states.

From a modelling perspective it is more difficult to obtain and fit a nonlinear model, especially if it contains an uncertainty description. More step tests would therefore be needed to obtain the uncertainty description. The nonlinear model presented in this study does contain model parameters that relate better to the physical process, which makes it easier to estimate bounds on the parameters from experience and other experiments than just step tests on the plant. The advantage of PI control is that it does not require an uncertainty description to design the controller. PI control therefore requires less engineering effort to design compared to RNMPC.

Online tuning of both the RNMPC and PI controllers would be required for best performance. Every time there is a change in the plant hardware, such as new instrumentation or actuators, recalibration of the model for the RNMPC as well as retuning of PI controllers would usually be required.

The cost of maintaining the nonlinear model may be reduced if the nonlinear model can be structured to have calibration parameters and process parameters. The calibration parameters can relate to gains of measurement equipment and gains of actuators. These calibration parameters can be assumed to be time-invariant and known. This will reduce the amount of work necessary for recalibration due to hardware changes.

However, the process parameters that relate to feed size distribution and ore hardness, for example, are specified as time-varying and uncertain. These process parameters would not need to be re-calibrated with changes in the process hardware, but would need to be re-calibrated for changes occurring in the process, such as a new type of ore being milled. The process parameters will require more effort to obtain, because uncertainty bounds would usually need to be established for these parameters.

The nonlinear model of the RNMPC is therefore more costly to commission and maintain compared to simple PI controllers. The cost of the hardware required to host the controller is also much higher. The feasibility analysis of using RNMPC compared to PI control will need to weigh the advantage that RNMPC can bring in terms of process performance against the added commissioning and maintenance costs.

The PI controllers presented in this thesis serve only as an example implementation to provide a baseline for comparison with RNMPC and NMPC. Single-loop PI controllers without a MIMO compensator were used, because more than 60% of all respondents still use PI controllers, according to a recent survey by Wei and Craig (2009), usually single-loop PI controllers. RNMPC and NMPC are, however, fundamentally different from single-loop PI controllers, because RNMPC and NMPC are multivariable, model-based controllers that can handle constraints explicitly, while single-loop PI controllers cannot handle multivariable interaction very well and only have constraint-handling capabilities through extensions, such as anti-windup. Single-loop PI controller design for multivariable systems with constraints is a complex field with a large number of issues and solutions. There are furthermore a number of different techniques to tune the controllers from Ziegler-Nichols, internal model control with SIMC (Skogestad, 2003) for example, to pole placement, etc. The PI controllers presented here are not intended to serve as the best PI controller design for the presented milling circuit based on an exhaustive study, because that was not the main focus of this thesis. The comparison of the RNMPC and NMPC controllers to the PI controllers should, therefore, not be seen as a definitive, but rather serve as an example of possible benefits that RNMPC can provide over PI control typically employed in industry (Wei and Craig, 2009), when large feed disturbances are common in the milling circuit.

The performance of the NMPC controller is very similar to the performance of the RNMPC controller. Some of the differences can be attributed to the ability of the RNMPC to handle rate constraints on the MVs. The RNMPC did not exhibit any significant stability or performance advantage in a majority of the simulations over the NMPC, which leads to the conclusion that the NMPC controller is more than adequate for controlling the ROM milling circuit presented here.

6.2 FURTHER WORK

The first barrier to the practical implementation of RNMPC is reducing the computational time. The computational time of the optimisation problem can be improved by

- decreasing the optimisation problem size, because the control algorithm is hampered mainly by a large number of slack variables for implementing robustness, but this will require simplifying assumptions to be made that can increase conservatism,
- replacing the nonlinear optimiser by a method that is less computationally expensive, or
- employing a nonlinear optimiser with better support for multiprocessor systems.

The real time iteration scheme developed by Diehl *et al.* (2005) allows the whole optimisation problem to be prepared before the state measurement is available, and only requires a small amount of time to finalise the calculation when the state measurement becomes available. It also performs only one iteration per interval, which gives it a very consistent calculation time that is very beneficial for practical control purposes.

The second barrier is the lack of an observer to allow for output feedback, rather than full-state feedback. The simulations were conducted with the assumption of full-state feedback, which is not possible in real life scenarios. A form of state estimation should be added to the loop to obtain a more accurate simulation of the closed-loop response. A classical extended Kalman filter can be used for state estimation or a form of moving horizon estimator. Moving horizon estimators are similar to MPC in principle and can easily be incorporated in the current framework. The moving horizon estimator could also include the nonlinear model directly rather than a linearised model, as will be needed by the extended Kalman filter. The amount of work to maintain different models for simulation, estimation and control will be reduced by using the nonlinear simulation model directly in the estimator as well as in the controller. For nonlinear systems this is more difficult, because the combination of the controller and observer should be stable.

The RNMPC presented in this study is based on open-loop min-max optimisation. There is a spread of possible future state trajectories when predicting the evolution of an uncertain system, which is the result of accounting for all possible realisations of the system owing to uncertainty in the model parameters, as well as the possible disturbances that might occur in future. The effects of feedback are not taken into consideration during predictions of future state trajectories in open-loop predictive control, which results in the state trajectories diverging more over the prediction horizon compared to closed-loop or feedback formulations. This increased spread in state trajectories will result in unnecessary conservatism and a reduced feasible region of the controller. The RNMPC can be modified to optimise over feedback laws that will result in a feedback robust nonlinear model predictive controller. The effects of feedback are then taken into consideration as part of the predictions, which will reduce the spread of state trajectory over the prediction horizon. This reduced spread of state trajectories compared to open-loop formulations has the result of an increased feasible region, reduced conservatism and increased performance of the controller.

Reduce the spikes in the manipulated variables by adding the appropriate rate constraints to the controller formulation that will not affect the stability properties of the controller (Mhaskar and Kennedy, 2008).